AD-A170 150 LARGE EDDY STRUCTURES IN TRANSITIONAL AND TURBULENT FLAMES(U) CARNEGIE-MELLON UNIV PITTSBURGH PA DEPT OF MECHANICAL ENGINEERING N CHIGIER 23 AUG 85 1/1

UNCLASSIFIED AFOSR-TR-86-0499 AFOSR-82-0266 F/G 21/2 NL

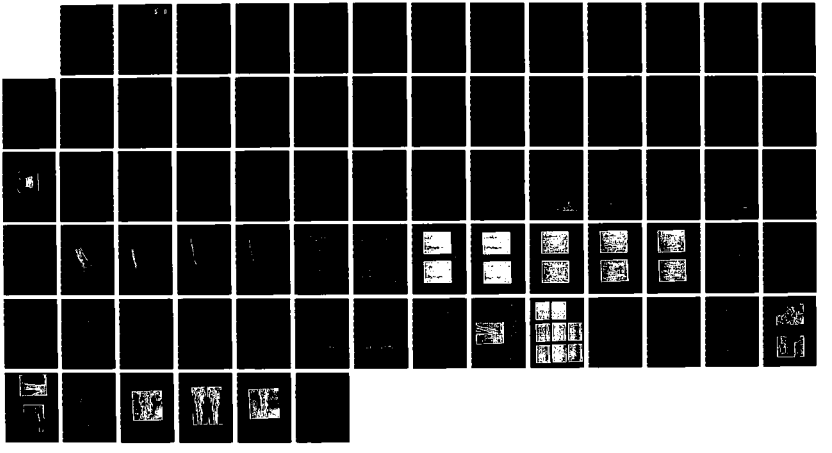

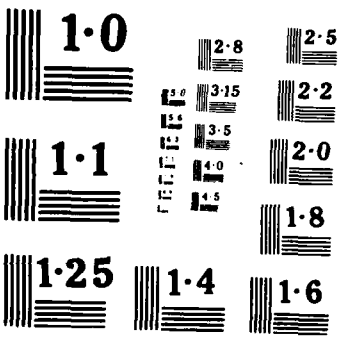
1·0
1·1
1·25
1·4
1·6
1·8
2·0
2·2
2·5
2·8
3·15
3·5
4·0
4·5
5·0

SECURITY CLASSIFICATION OF THIS PAGE

(2)

DTIC ELECTE JUL 25 1986 S D

REPORT DOCUMENTATION PAGE

AD-A170 150

1b. RESTRICTIVE MARKING: None	
2b. DECLASSIFICATION/DOWNGRADING SCHEDULE	3. DISTRIBUTION/AVAILABILITY OF REPORT: Unlimited
4 PERFORMING ORGANIZATION REPORT NUMBER(S)	5. MONITORING ORGANIZATION REPORT NUMBER(S): AFOSR-TR- 86-0499
6a. NAME OF PERFORMING ORGANIZATION: Carnegie-Mellon University; 6b. OFFICE SYMBOL (If applicable)	7a. NAME OF MONITORING ORGANIZATION: Air Force Office of Scientific Res.
6c. ADDRESS (City, State and ZIP Code): Mechanical Engineering Department, Pittsburgh, PA 15213	7b. ADDRESS (City, State and ZIP Code): Bolling AFB, D.C. 20332-6448
8a NAME OF FUNDING/SPONSORING ORGANIZATION: Air Force Office of Sci. Res.; 8b. OFFICE SYMBOL (If applicable): AFOSR /NA	9. PROCUREMENT INSTRUMENT IDENTIFICATION NUMBER: AFOSR 82-0266
8c ADDRESS (City, State and ZIP Code): Bolling AFB, D.C. 20332-6448	10. SOURCE OF FUNDING NOS.

PROGRAM ELEMENT NO.	PROJECT NO.	TASK NO.	WORK UNIT NO.
61102F	2308	A2	

11. TITLE (Include Security Classification): Large Eddy Structures in Transitional & Turbulent Flames(unclassified)

12. PERSONAL AUTHOR(S): Norman Chigier

13a. TYPE OF REPORT	13b. TIME COVERED	14. DATE OF REPORT (Yr., Mo., Day)	15. PAGE COUNT
Final	FROM 7/1/82 TO 6/30/85	8/23/85	76

16. SUPPLEMENTARY NOTATION

17. COSATI CODES			18. SUBJECT TERMS (Continue on reverse if necessary and identify by block number)
FIELD	GROUP	SUB. GR.	Large eddy structures, transitional jet flames, premixed and non-premixed diffusion flames
21	01		
21	02		

19. ABSTRACT (Continue on reverse if necessary and identify by block number)

An experimental investigation of transitional and turbulent jet diffusion flames, has been carried out with emphasis on the derivation of time-dependent information from measurements of various fluctuating quantities in these flames. Special efforts have been made to control carefully, and vary systematically, the initial and boundary conditions of each flame. The burner assembly consists of an interchangeable circular fuel burner and a secondary air supply system. The study began with a reexamination of the classic work of Hottel and Hawthorne which led to the discovery of a hysteresis phenomenon in the liftoff and reattachment of hydrocarbon flames. A laser-Doppler anemometry system has been developed that has the capability of sampling turbulent flows at a rate of nearly ten times that of more commonly used systems. Ionization and microthermocouple probes have been assembled that will prove invaluable for conditional

20 DISTRIBUTION/AVAILABILITY OF ABSTRACT	21. ABSTRACT SECURITY CLASSIFICATION
UNCLASSIFIED/UNLIMITED ☒ SAME AS RPT. ☐ DTIC USERS ☐	Unclassified

22a. NAME OF RESPONSIBLE INDIVIDUAL	22b. TELEPHONE NUMBER (Include Area Code)	22c. OFFICE SYMBOL
Julian M. Tishkoff	(202) 767-4935	AFOSR/NA

DD FORM 1473, 83 APR EDITION OF 1 JAN 73 IS OBSOLETE. Unclassified

SECURITY CLASSIFICATION OF THIS PAGE

DTIC FILE COPY

86 7 23 286

sampling. Finally, flow visualization has been accomplished through standard still photography, high-speed cinematography, and schlieren photography.

Ionization current measurements have been made in Methane and Propane jet diffusion flames using a Langmuir probe. Digital collection and analysis were accomplished by a MINC minicomputer, measuring the mean and RMS values of ion current. Power spectra analysis was also accomplished with Fast Fourier Transform (FFT) routines.

The mapping of the signal reveals that the inner flame boundary moves radially outward in the near flow-field (x/D=10 to x/D=40) and later converges toward the flame axis. Meanwhile, the outer flame boundary grows steadily with downstream (axial) distance, indicating a consistently widening reaction zone, for the entire area examined (x/D=10 to x/D=60).

Profiles of RMS values of ion current were also correlated with the flame boundary locations. A double peak pattern was found in the RMS profiles, each peak coinciding with the large gradients of the mean ion current profiles. Near the inner flame boundary, the flame front fluctuates across the probe's sampling volume, generating largely fluctuating components of ion current. These fluctuations manifest themselves as peaks on the RMS profiles. In the central flame region, the probe experiences a more continuous flame presence and less fluctuations. This causes the mean ion current signal to remain high while the RMS signal drops off rather rapidly. As the outer flame boundary is approached, an increase in fluctuations again takes place, which could be expected to produce a sharp increase in the RMS value. However, because the strength of the overall ion current signal weakens in this region, (mean current drops off significantly), the RMS value is smaller than would be expected. While points farther downstream do indeed show significant peaks on the outer boundary, the near flow fields do not display the characteristic second peak.

The ion current signal drop off could be caused by two sources of ion dilution. As radial distance increases larger amounts of air are entrained into the flame, causing a dilution of the ion concentration and a corresponding weakening of the signal. Secondly, the volume for ion occupation increases with the square of the radius allowing significant ion dilution to occur at the outer boundary.

Introduction

The understanding of the fluid dynamic structure of flames continues to be of importance in the design and development of burner systems used in industrial furnaces and combustion chambers. The round turbulent free jet flame may be considered the model of such systems. Previous work [2] has described the general appearance of the first fifteen diameters of a typical turbulent jet flame (Figures 3 to 5). Obtained from high-speed schlieren motion pictures, these sketches show a double structure consisting of inner, fast moving eddies and outer, larger, slow moving eddies. It is the growth, development, and interaction of these two structures that is the focus of this research. The primary goal is the development of conditional sampling techniques and their subsequent application to the examination of coherent structures in transitional and turbulent jet diffusion flames.The principle diagnostic techniques developed to achieve this goal include laser-Doppler anemometry, ionization probes, and fine wire thermocouples. The study began with a reexamination of the relationship between flame height and fuel flow rate.

Several students have worked on this research project. Tom Zsak obtained his masters degree and was awarded the Guggenheim Fellowship at Cal Tech to continue his Ph.D. studies. Caroline Perlee obtained her masters degree and is continuing her studies as a Ph.D. student in Electrical Engineering at Carnegie-Mellon University. Ken Laskey has moved on to computational work at NRL for his Ph.D. studies. Craig Niiya has graduated as a senior student in Mechanical Engineering. John Feeney and other members of the combustion research team have made contributions to the work reported.

Flame Height Measurements

A test of the integrated result of any detailed flame model is how well that model predicts the experimentally measured flame height. As a first step in this study, data were collected on hydrogen, methane, and propane flames at various flow rates and for various burner geometries.(Figs.1,2) In all cases, the flames were unconfined but surrounded by a coflowing air stream having a velocity of 0.5m/s. This simple geometry allows for the possibility of comparison with theories which produce analytically solvable differential equations. The measurements were taken visually and represent the average vertical distance between the nozzle exit and the flame tip. Becker and Liang [10] note that visual measurements of this type are most appropriate for collecting average flame height data.

It was expected that a detailed database could be produced that followed the pattern described by Hottel and Hawthorne [1] and included in many standard texts on combustion [3,4,9]. The classic Hottel and Hawthorne diagram appears in Figure 6. For low flow velocities, flame height increases linearly with exit velocity. As the exit velocity of the fuel increases, the flame height varies as the log of the volumetric flow rate, i.e. for a given diameter nozzle, the increase in the flame height with increasing velocity is less than linear. Both the linear and log-linear regions are described by Hottel and Hawthorne as "sharp-edged and constant in shape." In other words, they are laminar flames. Passed the log-linear region, the flame tip forms a "brush" and the transition to turbulence begins. The height of the "fully developed" turbulent flame is less than the maximum laminar height and constant. Figure 7 shows a comparison of data obtained in this study with that obtained by Hawthorne [6]. Note that the current data do not follow the trend previously described. A strictly linear tendency is shown at very low flow velocities in Figures 8 and 9, but no maximum is seen at

higher velocities. A linear trend may be found when the data are plotted on semilog axes using the log-linear variables suggested by Hottel and Hawthorne for the second laminar regime (Figure 10). Much of the data contained in this plot, however, is not only for the laminar flames studied but also for flames stabilized above the nozzle exit. These "lifted" flames were not addressed by Hottel and Hawthorne. Given this unexpected inconsistency, an examination of the literature was undertaken to compare the data with other published results and to look for a resolution to the disagreement.

Figure 11 contains data from four studies including the present one. For the smaller diameter burners, the data do show a slight decrease from a maximum height (References 7 and 8 do not comment on whether this maximum occurs for a laminar flame before transition) to a constant value independent of fuel velocity. For moderate and larger diameter nozzles, this maximum is not in evidence; however, the trend toward increasing flame height with increasing burner diameter for constant exit fuel velocity is consistent in this plot. Similar results can be seen in Figure 12 for propane.

The most complete explanation for the collected data appears in two articles by Baev and coworkers [7,8]. In Figure 13a, one can see the classic curve described by Hottel and Hawthorne. This result was derived by Baev in the absence of lifting forces, i.e. for flames with an infinite Froude number, Fr. Theoretically, the maximum laminar height could exceed the constant turbulent height by a factor of 1.74. For lesser, though still large values of Fr, the sketch in Figure 13b shows that the "hump" of the flame height curve will decrease and eventually vanish. Figure 13c shows this same tendency but in terms of the nozzle

diameter. Thus for small diameter nozzles, the flame height, which scales almost linearly with Reynolds number, Re, at low Re, increases past the constant high Re height and then decreases after transition to a value below the constant height before approaching the final constant value asymptotically. The ratio of maximum flame height to constant high Re height decreases with increasing nozzle size as the effects of buoyancy become more pronounced, that is, Fr increases. For nozzle diameters greater than some critical value, the flame height never exceeds the high Re value but approaches it asymptotically from below. The data of the present study plotted in Figure 14 agrees qualitatively with this argument.

In the presence of lifting forces and for small values of Re, Baev suggests the correlation

$$L/d \cong Re^{2/3} Fr^{1/3} \cong u^{4/3} d^{1/3}$$

where L = flame height
d = nozzle diameter
u = exit fuel velocity

The log-log plot in Figure 15 shows that much of smaller value data does fall along a curve with slope equal to unity and thus shows agreement with this correlation.

For higher values of Re and correspondingly higher values of Fr, many sources [7,11,12] correlate the data by the following:

$Fr < Fr^*$

$$L/d = A\, Fr^m, \quad m = 0.2$$

$Fr > Fr^*$

$$L/d = A$$

Although this form does not appear explicitly in References 7 and 8, the suggested variable groupings in those analyses can be reduced to this Froude number form with the remaining variables providing expressions for the constant coefficient A. Figure 16 shows this study's data plotted as L/d versus Fr. Most of the data appears to fall along a line having a slope of approximately 0.2. The lower values which do not fit this slope were correlated in Figure 15, and the higher values approach a constant value. Figures 17 and 18 show the various collected data plotted in this manner.

The accomplishment of this flame height study has been twofold. First, a large amount of data taken under carefully recorded conditions has been added to the body of literature. Secondly, consistency has been shown to exist in a large body of data, and an explanation of those data beyond the most widely quoted source has been indicated. It was during this study that an interesting discovery was made dealing with the liftoff and reattachment of methane and propane flames.

Flame Height Hysteresis

The subject of lifted turbulent jet diffusion flames has enjoyed a renewal in interest lately, primarily due to the work of Peters and Williams [13]. In the mid-1960's, Vanquickenborne and van Tiggelen [14] put forth the most widely accepted explanation for the stabilization mechanism of these flames. This mechanism is dependent on the entrainment of surrounding air into the non-burning part of the gas jet between the burner and the base of the flame. At the base, a "premixed region" forms, and stabilization occurs at a point where the local cold flow velocity is equal and opposite to the local turbulent flame speed. Doubting the extent of premixedness, Peters and Williams suggest that the lifted flame is made up of a number of laminar diffusion flamelets and that stabilization occurs at the last downstream position where these flamelets are locally quenched by excessive mixing [15]. The existence of a series of small scale eddy-flames and large scale lump-flames containing a definite number of eddy-flames has been confirmed at the base of a turbulent flame prior to and after liftoff by Yamaguchi and coworkers [16].

The following data illustrate an interesting hysteresis phenomenon associated with the liftoff and reattachment of hydrocarbon flames that has not been reported in the literature save for a comment by Eickhoff at the Nineteenth Symposium (International) on Combustion [5].

In the present study, flames fueled either by methane or propane were found to lift from the burner upon steadily increasing the fuel flow rate. Liftoff was found to occur at a nozzle exit fuel velocity of 14.7m/s (Re = 15920) for propane and at 21.4m/s (Re = 6359) for methane.

These flames were initially stabilized on a circular nozzle having an exit diameter of 5mm. As the fuel flow rate increased, the attached flames stretched, became perforated, and then completely detached from the burner rim at sudden liftoff. Once lifted, a continued increase in fuel flow resulted in an increase in both the visible flame height and the position of the base of the flame above the nozzle. A decrease in fuel flow caused the flames to reattach to the burner rim. This occurred at an exit fuel velocity of 4.81m/s (Re = 5139) for propane and at a velocity of 6.25m/s (Re = 1857) for methane. Within the hysteresis region, bounded by the velocities of liftoff and reattachment, flame heights were significantly shorter while decreasing the flow for a lifted flame as compared to increasing the flow for an attached flame. Once reattachment had occurred, flame length suddenly increased to the value of the initial rim-stabilized flame. The flame height variations had the characteristics of a hysteresis loop, and the results were reproducible and independent of the time between measurements and the rate of change of fuel flow. Figures 19 to 22 illustrate this phenomenon. A hysteresis loop was not observed for hydrogen flames, for liftoff could not be achieved at fuel velocities of up to 104m/s (Re = 4851).

Photographs of propane flames within the hysteresis loop of Figure 21 are shown in Figures 23 to 27. In each figure, the pair of flames on the left were photographed at a shutter speed of 1/1000th of a second and the pair on the right had an exposure of 1/60th of a second. As one can see from the photographs having the shorter exposure time, the structures of the attached and lifted flames are very similar, although the attached flames are slightly more luminous especially at the higher flow velocities. These structures are very much like those reported by Chigier and Yule [17], and the flames do in fact appear to be "nicked" into dis-

crete "chunks."

Since the flames' movements are frozen at an exposure of 1/1000th of a second, flame height is not accurately represented and a much longer exposure is necessary to record the flame tip fluctuations. A shutter speed of 1/60th of a second was therefore chosen. From these pairs of photographs in Figures 23 to 27, one can see the flame height differences within the hysteresis loop. It is clear that for a given fuel velocity the lifted flames are shorter than their corresponding attached flames. This difference increases as the fuel velocity tends to the lower bound or reattachment velocity.

Additionally, the secondary air velocity was varied while flames were lifted to examine the influence of jet-to-stream velocity. It was found that the stabilization positions of the flames increased in height above the nozzle as the secondary air velocity increased. Typical results are given in Figure 28 for propane flames at various exit velocities.

It was expected that the occurrence of liftoff would be sensitive to burner exit conditions. More specifically, would the presence of recirculation zones at the nozzle exit affect the liftoff process? Generating recirculation at the burner port by attaching annular disks at the exit showed that the stronger the recirculation zone present, the longer the flames were able to remain stabilized on the burner rim as the fuel velocitiy increased. The liftoff position was also sensitive to the presence of recirculation until the fuel velocity reached a certain value where this position was independent of the strength of the recirculation zone. This is shown in Figure 29.

Velocity measurements were made within the flames shown in Figure 23

by the laser-Doppler anemometry system shown in Figure 30. The results, given in Figures 31 to 33, show the variations in flow field structure and turbulence characteristics at several axial positions. The effect of combustion on the mean velocity is clearly evident in Figure 31. The lifted flame exhibits free-stream velocity decay along the axis as expected, for the flame is stabilized at 15 to 17 diameters downstream of the burner port. For the attached flame, however, there is very little axial velocity decay even at the position 15 diameters downstream. Combustion, therefore, has extended the potential core of the fuel stream. Little can be said of the turbulence data given in Figures 32 and 33 since the points are so scattered. This almost random quality may be the result of non-steady seeding rates from the fluidized bed seeders used to introduce alumina particles to both the fuel and secondary air streams. The examination of flame height hysteresis led to the first application of the laser anemometry system developed at Carnegie-Mellon, and it is in this area that significant developments have occurred.

Laser Anemometry in Flames

Research at Carnegie-Mellon University in laser-Doppler velocimetry, LDV, measurements has resulted in the development of software specifically designed for high-speed data acquisition so as to allow high frequency recording of velocity as a function of time for conditional sampling. The software is compatible with both the PDP-11/34 and MINC-23 minicomputers currently being used at the University. All data acquisition is done by way of Direct Memory Access, a high-speed form of data transfer. Because of this, the system developed in this research is capable of measuring velocity fluctuations occurring at frequencies up to 67kHz, that is, the system has the capability of sampling velocities within the flame at a rate of almost 140kHz. By comparison, other commonly used methods of data transfer in LDV systems operate at sampling rates less than 15kHz. The graphical support for the system includes a time-history plotting package, which provides a plot of the acquired velocities versus their time of acquisition allowing conditional sampling and detection of flow structures, and a histogram plotting package which displays the estimated probability of occurrence of a specific range of velocities.

The LDV optics used in this study are commercially available from TSI Incorporated and are shown, once again, in Figure 30. As can be seen, the arrangement is a single color system based on a 15mW He-Ne laser and is capable of measuring one velocity component, in this case, the axial component, in the flame under study. Due to the fact that the research at Carnegie-Mellon has resulted in a sampling rate of nearly ten times that of commercially availble systems, it is now possible to follow the very rapid velocity fluctuations common in turbulent flames making the system well suited for combustion studies. The conclusions to be drawn from this work are [18]:

1. Direct Memory Access can be used with LDV systems to provide data-acquisition rates many times those of other commonly used methods of data transfer including digital input by programmable I/O.
2. The rate of data transfer in actual LDV measurements depends on the particle concentration within the flow. However, provided the particles are arriving at the measurement volume at an adequate rate, the Direct Memory Access method is capable of detecting velocity fluctuations at frequencies up to 67kHz corresponding to an average time-between-data of approximately 7.5μs.
3. Several programs have been created to perform a variety of software functions with the intention of using the LDV data in conditional sampling of various flame properties.

The concept of conditional sampling, introduced in the analysis of non-periodic functions of time, is not new to turbulent flow studies. It is new, however, in its application to LDV measurements. The purpose of conditional sampling is to reveal "interesting" features that appear intermittently rather than continuously. In general, it is necessary to specify in advance what instantaneous properties of the signal are considered "interesting" though any measurable property may be chosen.

Figure 34 illustrates an example of conditional sampling in a flow whose velocity measurements are continuous with time (such as from a hot-wire anemometer). The data of Figure 34a represent velocity measurements at a flow location A. If high frequency turbulence is of interest in this case, the conditioning criterion may be chosen such that the conditioned data of Figure 34b result, that is, only those turbulent frequencies that satisfy the criterion remain. The conditioning function of Figure 34c is then formed from the results of Figure 34b and the data from all other simultaneous flow measurements, such as the velocities of Figure 34d, are then conditioned by way of the function of Figure 34c

producing the data of Figure 34e. Now only the "interesting" data given in Figures 34b and 34e remain to be analyzed.

A useful tool to determine what features are interesting is some form of picture showing certain flow properties as they vary with time. Such a tool for displaying the variations of velocity within transitional and turbulent flames has been created in this research. It is a time-history plot of the sampled data whose purpose is to show the velocity variations with time at some location within the flame. This plot allows the experimenter to visualize actual flow fluctuations and to determine what, if any, interesting features exist.

Figures 35 and 36 show typical output obtained from LDV measurements within a propane flame having an exit Reynolds number based on cold flow conditions of approximately 14000. The velocities reported are in the axial direction. Each figure contains a time-history plot of a particular set of 512 velocity samples taken from a total of 2560 available samples. As one can see, the velocity fluctuations are roughly 3% of the mean in both cases. This low level of turbulence intensity is to be expected since the measurements were taken just above the nozzle port. Remember, the nozzle is contoured to provide a uniform velocity profile at its exit. The large velocity excursions below the mean were not expected. They have been determined to be the result of the inability of larger seeding particles to follow the accelerations of the surrounding fluid. As can be imagined, the time-history plots are invaluable to an experimentor wishing to identify periodic flow structures, and when used in conditional sampling, they will reduce the risk of choosing a criterion that has no relevance to the flow under study.

Ionization and Microthercouple Probes

In order to facilitate the study of the growth, development, and subsequent history of the eddy structures depicted in Figures 3 to 5, a probe able to follow the time-dependent phenomena associated with flame presence had to be incorporated into the experimental program. Such a probe could be used as a triggering mechanism for other instruments and would prove quite valuable when carrying out conditional sampling. One such device is the ionization probe, for it is sensitive to the ions existing in the reaction zone and possesses adequate spatial resolution and time response.

It is well known that the peak ion density closely follows the reaction zone. This is due to the fact that the recombination time of ions (10^{-7} to 10^{-5} seconds) is at least one order of magnitude shorter than the time scale of fluctuations in turbulent flames [19]. As a consequence, diagnostic techniques based on ionization are appropriate tools for the examination of flame turbulence [20].

The principle of operation of the ionization probe is fully treated in the literature [21], and a review of the theories supporting the use of the probe has been written by Smy [22]. Work using the ionization probe in the study of flame turbulence was first presented by Karlovitz and coworkers [23] at the Fourth International Combustion Symposium. Their study dealt with a natural gas/air premixed flame and measured the fraction of time the flame spent at the probe position, the most probable position of the combustion wave within the flame brush, and the rms displacement from this point. They also used the probe to detect "holes" in the flame which they related to the fullness of the flame. One of the more interesting studies in recent times using ionization probes in premixed flames was performed by Suzuki et al. in 1979 [24]. Here, two

sensors were used in premixed propane/air flames and the signals were cross-correlated to yield the most probable direction and velocity of local flame front movements. In fact, the vast majority of ionization probe studies have dealt with premixed flame situations. Detailed measurements in diffusion flames have only been realized by Lockwood and Odidi [25] and Ahlheim and Günther [26]. This paucity of literature dealing with diffusion flame ionization is one of the factors motivating the research at Carnegie-Mellon.

A typical probe used in the present study is illustrated in Figure 37. Its components include:

* sensor: Pt/13%Rh wire, 200μm diameter and 1.5mm exposed length
* probe body: standard 1/4" stainless steel tubing
* ceramic sheath: insulates wire from probe body

The sensing wire runs the length of the probe body to a connecting socket where coaxial cable carries the signal to the instrumentation. A diagram of the complete circuit is given in Figure 38. The voltage divider shown is necessary because the voltages produced by flame ionization are, in many cases, greater than the 5.12V threshold of the MINC-23 A/D converter. Once digitized, the signals are stored and processed using the MINC-23 minicomputer. To date, efforts in this study have been concentrated on obtaining mean and rms profiles of the ion signal in various methane and propane flames. Additional measurements to be carried out include peak analysis of the fluctuating signal, probability density function (pdf), spectrum and autocorrelation of the signal, and the cross correlation of the signals from two probes with axial and/or radial separation.

Figure 39 contains a photograph of a single probe in a lifted methane flame (Re = 3655) and a chart recording of a typical signal produced

when the fluctuating flame front comes into contact with the sensor. This contact results in the series of voltage peaks shown. The frequency of contact depends on the location of the probe within the flame as illustrated in Figure 40. Here, a sequence of oscilloscope traces are shown which follow the movement of the probe through the reaction zone of a methane flame (Re = 2960) at a distance of four diameters above the nozzle port. Photograph 40a was taken when the sensor was on the nozzle axis and surrounded by the cold fuel stream. At this location, there is no flame front present. Movement away from the axis results in the increased frequency of contact between the flame and probe resulting in a number of voltage peaks that are quite periodic (photographs 40b to 40f). Obviously, the probe is "seeing" the passage of eddy structures such as those depicted in Figures 3 and 4. As the probe passes beyond the reaction zone, activity ceases (photographs 40g and 40h). The dominant frequencies in signals such as those above can be obtained by power spectra analyses, and these can be related to the arrival of burning structures at the probe sensor. Taking the inverse Fourier transform, which is the autocorrelation of the signal, will permit the calculation of integral time scales.

Mean and rms voltage profiles of a turbulent propane diffusion flame (Re = 8853) are shown in Figures 41 and 42 respectively. In each case, 10 volts corresponds to roughly 0.1 microamps, and the nozzle rim is located at a radial position of 0.5 diameters. Figure 41 shows that the mean voltage drops sharply as the probe passes from the reaction zone into the surrounding air stream. As expected, this drop occurs further from the axis as axial distance is increased. This is due to the natural spreading of the flame. The inner and outer boundaries of the reacting interface can be determined from the locations of the dual peaks in rms voltage present at each axial position as shown in Figure 42. It can be

seen that the inner boundary moves toward the axis as axial distance increases while the outer boundary of the interface moves away. Profiles such as these allow one to determine the approximate shape of the flame under investigation quite readily.

Multiple probes are useful in examining the development and evolution of distinguishable features of flames. For example, signals from a pair of ionization probes could be used to follow the downstream movements of identifiable structures and cross-correlations could be obtained. Figure 43 is a chart recording of signals from two sensors located at an axial distance of 250 diameters and separated by a distance of a single diameter. The flame under investigation is the same propane flame mentioned when discussing the previous two figures. The spikiness of each signal and the dissimilarity between the two indicate the influence of turbulence on the flame structures.

The most suitable technique currently available for measurement of the local fluctuating temperature in turbulent combustion flows is generally accepted to be the use of unshielded, noble metals fine wire thermocouples. Since such fluctuations are of high frequency, thermocouple time response is at a premium, and wires of diameters of 25 to 75 microns must be utilized. Efforts at Carnegie-Mellon have concentrated on the construction of such thermocouple probes. Figure 44 displays the thermocouple welding station and Figure 45 shows two 25μm wires (Pt and Pt/13%Rh) prior to welding. The welded junction of these wires is shown in Figure 46. For comparison, a paper clip, having a diameter of 1000μm, is also present in the photograph. Finally, the thermocouple-to-support wire weld is shown in Figure 47. The support wires have diameters at least four times those of the thermocouple wires. Plans are being made to obtain temperature profiles in various jet flames using the MINC-23 minicomputer

and to use the thermocouples in conjunction with the ionization probes already assembled. To date, however, no temperature measurements have been made.

Schlieren

Along with standard still photography and high-speed cinematography, schlieren photography has been employed as a method of flow visualization. The technique known as "Rainbow Schlieren" [27] had been adapted to the experimental setup during the summer of 1983. A standard Z-type configuration was arranged and is depicted in Figure 48. Its components were:

* two 12in diameter spherical mirrors each having a focal length of 12ft
* 162W mercury arc lamp
* rainbow aperture

This technique is termed "rainbow" schlieren because a rainbow-like aperture is placed at the focal point of the imaging mirror. This aperture is a 35mm slide of concentric rings of color, the core being clear surrounded by rings of blue, green, yellow, orange, and red. Density differences in the flame are indicated by different colors in the schlieren image produced by varying degrees of light deflection through the flame test section. Black-and-White schlieren images were also produced by replacing the arc lamp and rainbow aperture with the 15mW He-Ne laser used in the LDV system and a dual knife-edge respectively. Examples of the black-and-white images are shown in Figures 49 to 51. Though it is difficult to detect flame structures in these photographs due to the poor quality of reproduction, one can nevertheless recognize the vortex formation in the outer flow around each flame just as depicted in Figure 5.

Conclusion

Research in the area of transitional and turbulent jet diffusion flames at Carnegie-Mellon began with a reexamination of a classical flame height study and has led to the development of several diagnostic techniques that make possible the application of conditional sampling. These include a laser-Doppler anemometry system capable of sampling a turbulent flow every 7.5 s and a number of ionization and microthermocouple probes. Immediate plans for the continuation of this study include:

* additional mean and rms ion profiles of fluid dynamically similar methane and propane diffusion flames
* velocity profiles of these flames to examine the relationships between fluctuations in velocity, temperature, and flame front location
* simultaneous measurements of ionization and temperature
* assemblage of a more sensitive schlieren system so that flow disturbances caused by the probes can be examined
* superposition of ionization probe oscilloscope tracings on high-speed schlieren motion pictures to relate signal shape to the type of structure passing the probe

With the present experimental program in operation, it is felt that significant contributions to the study of transitional and turbulent jet diffusion flames can be made at Carnegie-Mellon.

Publications and Presentations

Three papers dealing with this study were presented at the 1984 Fall Technical Meeting of the Eastern Section of The Combustion Institute held December 3-5, 1984 in Clearwater Beach, Florida. They were:

* Laskey, K., Zsak, T., and Chigier, N., "Variations in Height of Laminar and Turbulent Flames," Paper 4, Section A-1.
* Zsak, T., Perlee, C., and Chigier, N., "Hysteresis in the Liftoff and Reattachment of Hydrocarbon Flames," Paper 6, Section A-1.
* Perlee, C., Zsak, T., and Chigier, N., "Conditional Sampling by Laser Anemometry in Flames," Paper 18, Section A-3.

The following paper will be presented at the Western States Section of the Combustion Institute Fall Meeting at the University of California/ Davis, October 21/22, 1985:

Zsak, T.W., Niiya, C.K. and Chigier, N., "High Frequency Ionization Measurements in Diffusion Flames".

Dr. Chigier has visited and presented seminars at the Wright Patterson Air Force Base.

References

1. Hottel, H. C. and Hawthorne, W. R., "Diffusion in Laminar Flame Jets," Third Symposium on Combustion, Flame, and Explosion Phenomena, The Williams and Wilkins Company, 1949, pp. 254-266.
2. Chigier, N. A. and Yule, A. J., "Coherent Structures in Turbulent Flames," Interim Scientific Report, AFOSR Contract Number 77-3414, August 1978 - August 1979.
3. Kanury, A. M., Introduction to Combustion Phenomena, Gordon and Breach, New York, 1975.
4. Strehlow, R. A., Fundamentals of Combustion, International Textbook Company, Scranton, Pennsylvania, 1968.
5. Janika, J. and Peters, N., "Prediction of Turbulent Jet Diffusion Flame Lift-Off Using a PDF Transport Equation," Nineteenth Symposium (International) on Combustion, The Combustion Institute, 1982, pp. 367-374.
6. Hawthorne, W. R., Doctor of Philosophy Thesis, Massachusettes Institute of Technology.
7. Baev, V. K. and Yasakov, V. A., "Influence of Buoyant Forces on the Length of Diffuse Flames," Combustion, Explosions, and Shock Waves, 10, 1974.
8. Baev, V. K., Kuznetsov, P. P., Magil'nyi, I. A., Tret'yakov, P. K., and Yasakov, V. A., "Length of Diffusion Flames," Combustion, Explosions, and Shock Waves, 10, 1974.
9. Lewis, B. R. and von Elbe, G., Combustion, Flames, and Explosions of Gases, Academic Press, New York, 1961.
10. Becker, H. A. and Liang, D., "Visible Length of Vertical Free Turbulent Diffusion Flames," Combustion and Flame, 32, 1978.
11. Steward, F. R., "Linear Flame Heights for Various Fuels," Combustion and Flame, 8, 1964.
12. Heskestad, G., "Luminous Heights of Turbulent Diffusion Flames," Fire Safety Journal, 5, 1983.
13. Vanquickenborne, L, and van Tiggelen, A., "The Stabilization Mechanism of Lifted Diffusion Flames," Combusition and Flame, 10, 1966.
14. Peters, N. and Williams, F., "Liftoff Characteristics of Turbulent Jet Diffusion Flames," AIAA J., 21, 1983.

15. Sobiesiak, A. and Brzustowski, T. A., "Some Characteristics of Lifted Turbulent Jet Diffusion Flames," Fall Technical Meeting, Paper 5, Eastern Section of the Combustion Institute, December 3-5, 1984.

16. Yamaguchi, S., Ohiwa, N., and Hasegawa, T., "Structure and Blow-Off Mechanism of Rod-Stabilized Premixed Flames," Combustion and Flame, submitted for publication October 1984.

17. Chigier, N. A. and Yule, A. J., "The Physical Structure of Turbulent Flames," AIAA Paper 79-0217, Seventeenth Aerospace Sciences Meeting, New Orleans, Louisiana, January 15-17, 1979.

18. Perlee, C. J., "A Laser-Doppler Velocimetry System for High-Speed Acquisition and Conditional Sampling in Turbulent Flames," Master of Science Thesis, Carnegie-Mellon University, 1984.

19. Chomiak, J., "Application of Chemiluminescence Measurement to the Study of Turbulent Flame Structure," Combusition and Flame, 18, pp. 429-433.

20. Ventura, J., "An Experimental Study of the Transition to Turbulence in Propane Flames," Doctor of Philosophy Thesis, University of Sheffield, 1981.

21. Travers, B. and Williams, H., "The Use of Electrical Probes in Flame Plasmas," Tenth Symposium (International) on Combustion, The Combustion Institute, 1965, p. 657.

22. Smy, P. R., "The Use of Langmuir Probes in the Study of High Pressure Plasmas," Advances in Physics, 25, 5, p. 517.

23. Karlovitz, B., Denniston, D. W., Knapschaefer, D., and Wells, F., "Studies on Turbulent Flames," Fourth Symposium (International) on Combustion, The Williams and Wilkins Company, 1953, p. 613.

24. Suzuki, T., Hirano, T., and Tsuji, H., "Flame Front Movements of a Turbulent Premixed Flame," Seventeenth Symposium (International) on Combustion, The Combustion Institute, 1979, p. 289.

25. Lockwood, F. and Odidi, A., "Measurement of Mean and Fluctuating Temperature and Ion Concentration of Round Free-Jet Turbulent Diffusion and Premixed Flames," Fifteenth Symposium (International) on Combustion, The Combustion Institute, 1975, p. 561.

26. Ahlheim, M and Günther, R., "Ionization Measurements in Free-Jet Diffusion Flames," Combustion and Flame, 36, pp. 117-124.

27. Howes, W. L., "Rainbow Schlieren," NASA Technical Paper 2166, May 1983.

List of Figures

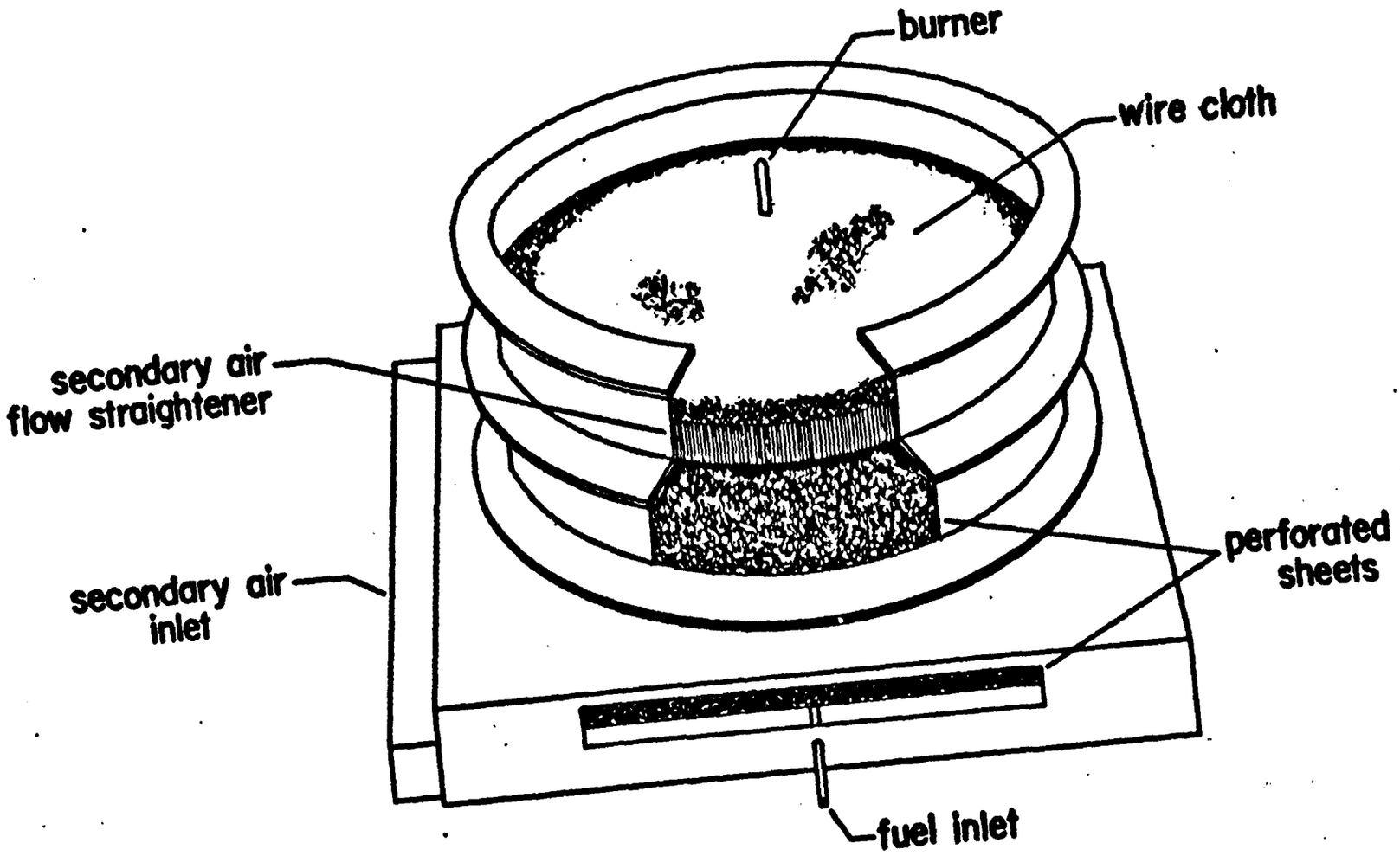

BURNER ASSEMBLY

Figure 1

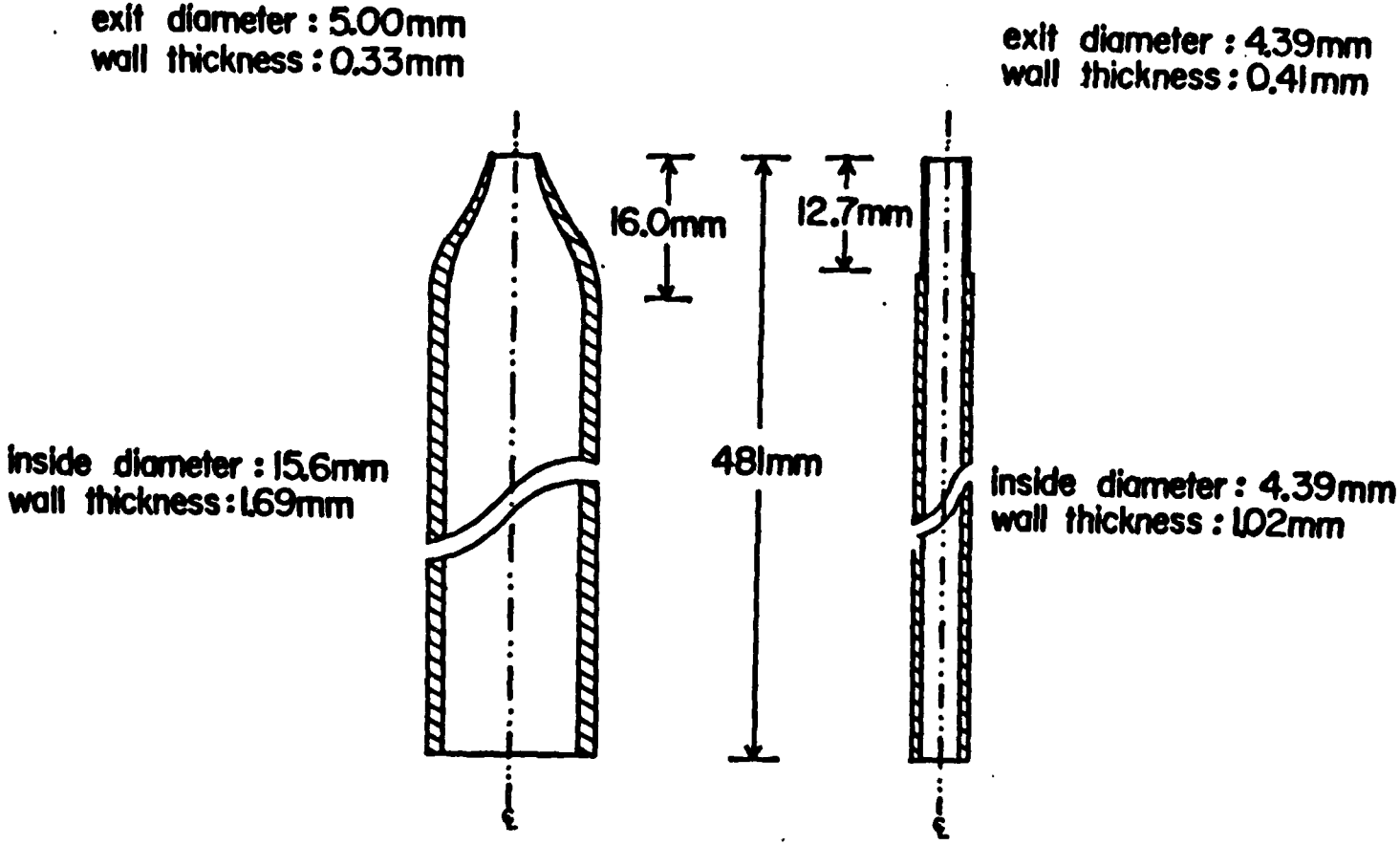

STAINLESS STEEL FUEL NOZZLE and TUBE

Figure 2

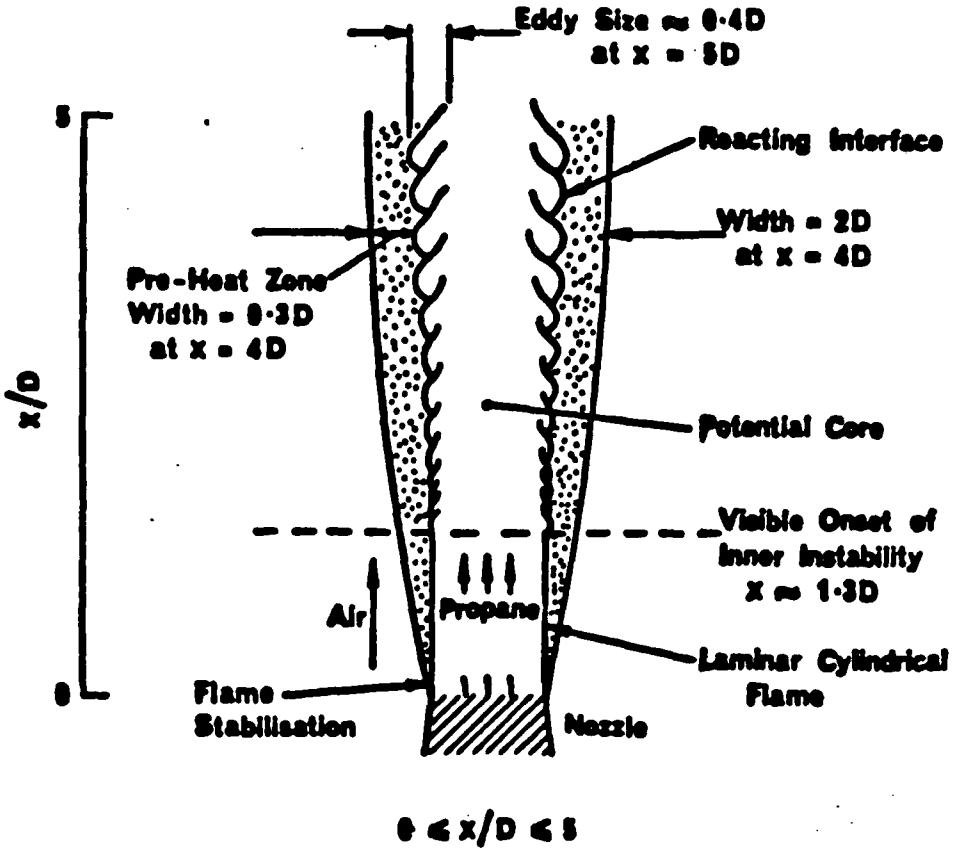
Eddy Size ≈ 0·4D
at x = 5D
5
x/D
0
Reacting Interface
Width = 2D
at x = 4D
Pre-Heat Zone
Width = 0·3D
at x = 4D
Potential Core
Visible Onset of
Inner Instability
x ≈ 1·3D
Air
Propane
Laminar Cylindrical
Flame
Flame
Stabilisation
Nozzle
0 ≤ x/D ≤ 5

Figure 3

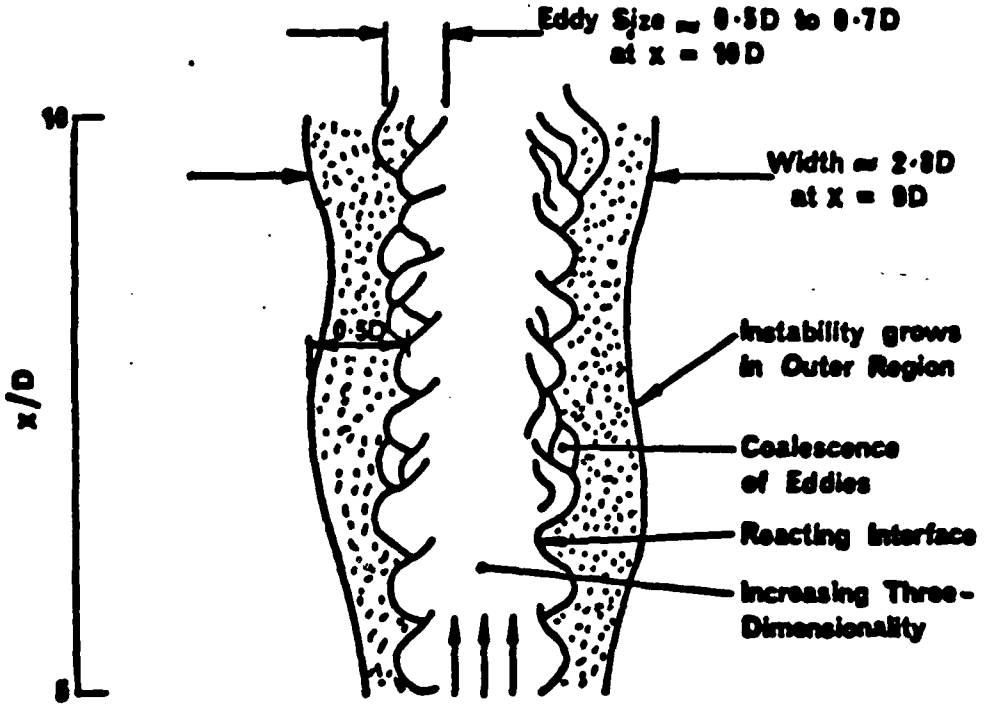
Eddy Size ≈ 0·5D to 0·7D
at x = 10D
10
Width ≈ 2·8D
at x = 9D
0·5D
x/D
Instability grows
in Outer Region
Coalescence
of Eddies
Reacting Interface
Increasing Three-
Dimensionality
8
8 ≤ x/D ≤ 10

Figure 4

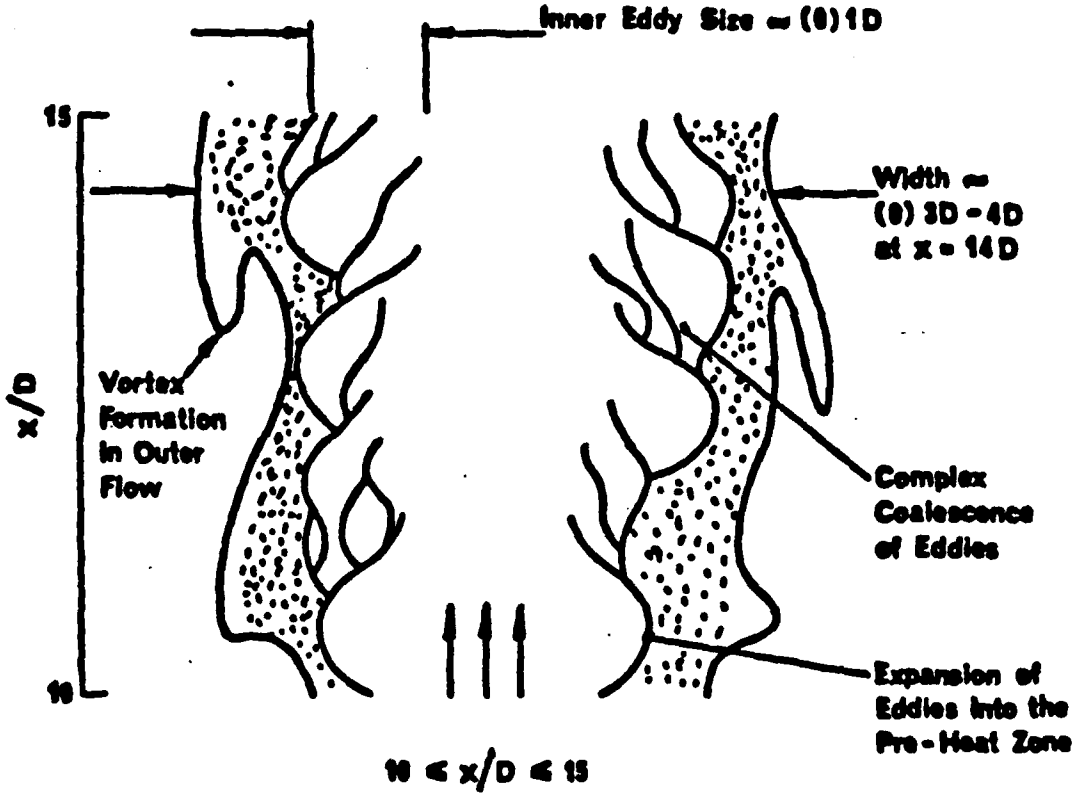
Inner Eddy Size ≈ (0) 1D
15
x/D
10
Vortex Formation in Outer Flow
Width ≈ (0) 3D - 4D at x = 14D
Complex Coalescence of Eddies
Expansion of Eddies into the Pre-Heat Zone
10 ≤ x/D ≤ 15

Figure 5

Hottel and Hawthorne

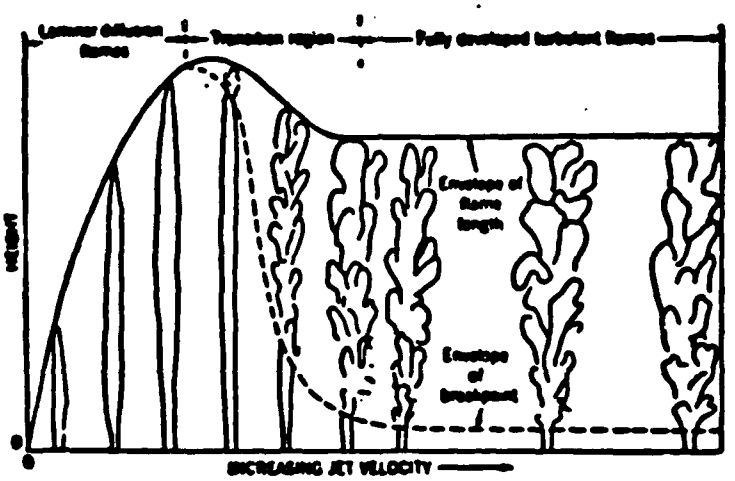

Figure 6

FLAME HEIGHT VS.FUEL VELOCITY FOR VARIOUS FUELS

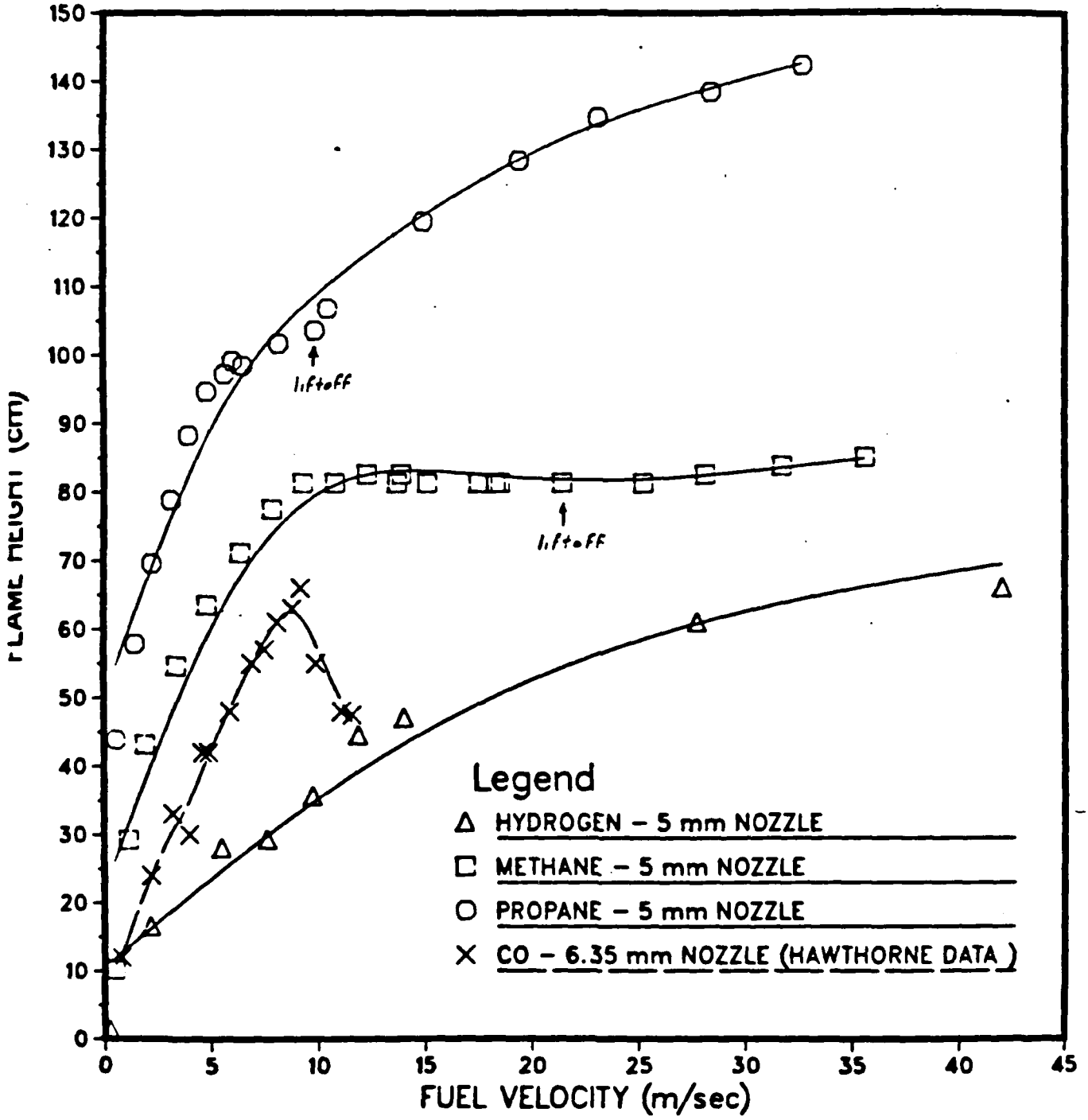

Figure 7

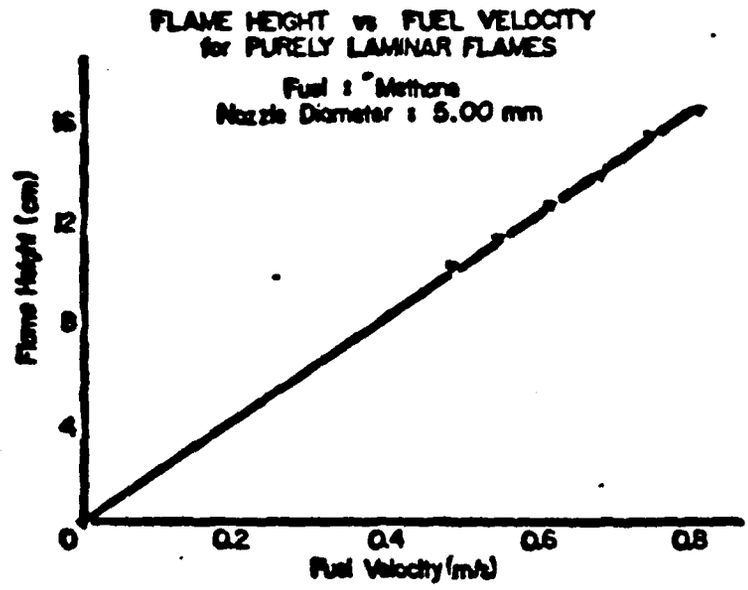

Figure 8

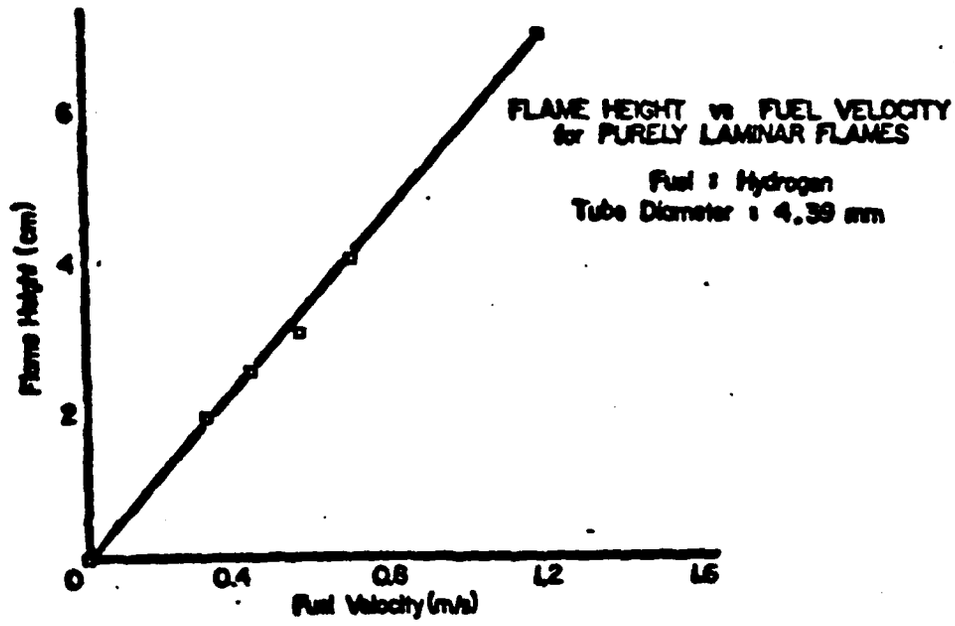

Figure 9

COMPARISON OF DATA WITH THOSE OF HOTTEL AND HAWTHORNE FOR CITY GAS AND CO FLAMES

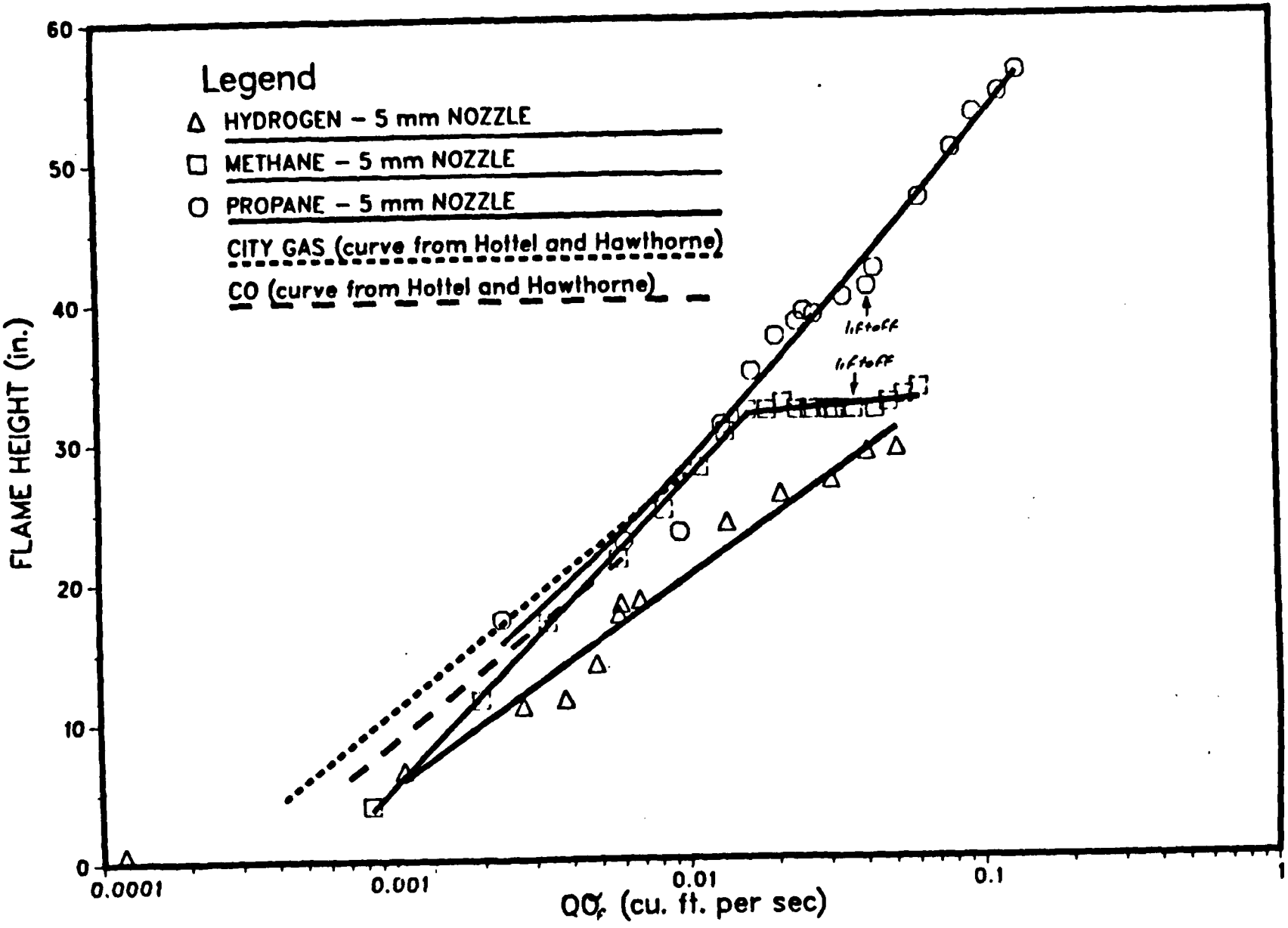

Figure 10

COMPARISON OF VARIOUS HYDROGEN DATA

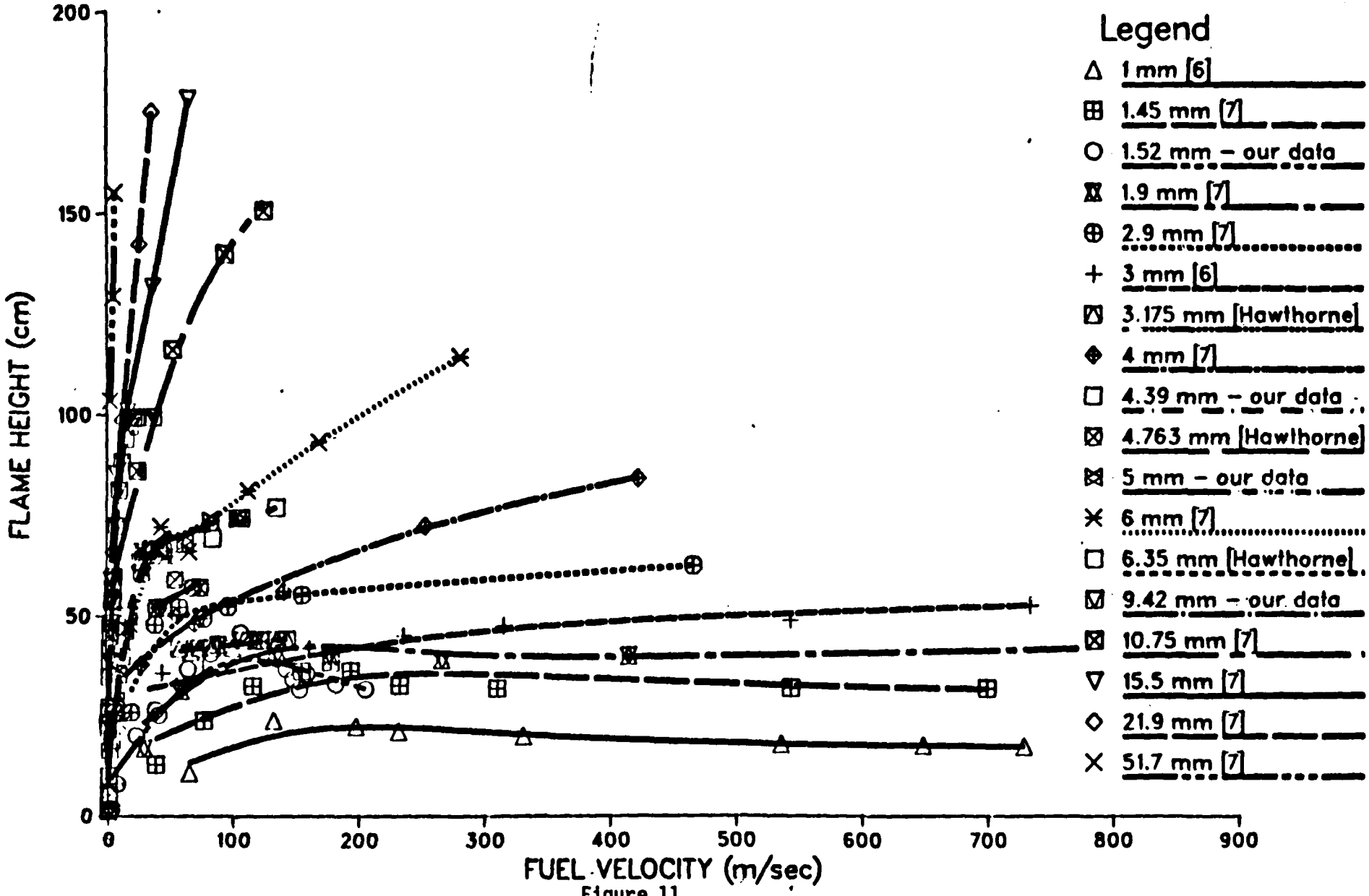

Figure 11

COMPARISON OF VARIOUS PROPANE DATA

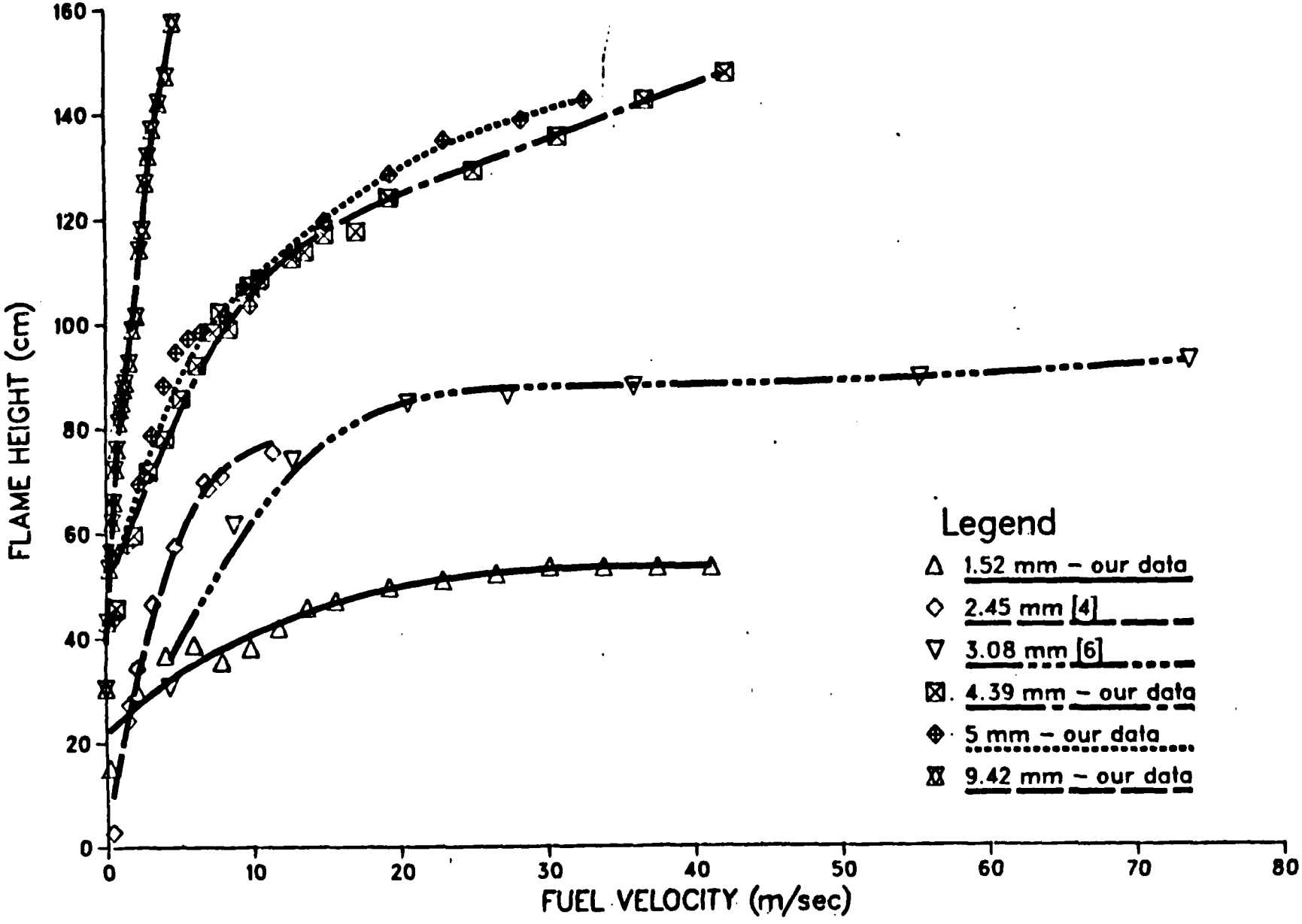

Figure 12

Baev, et. al. (1974)

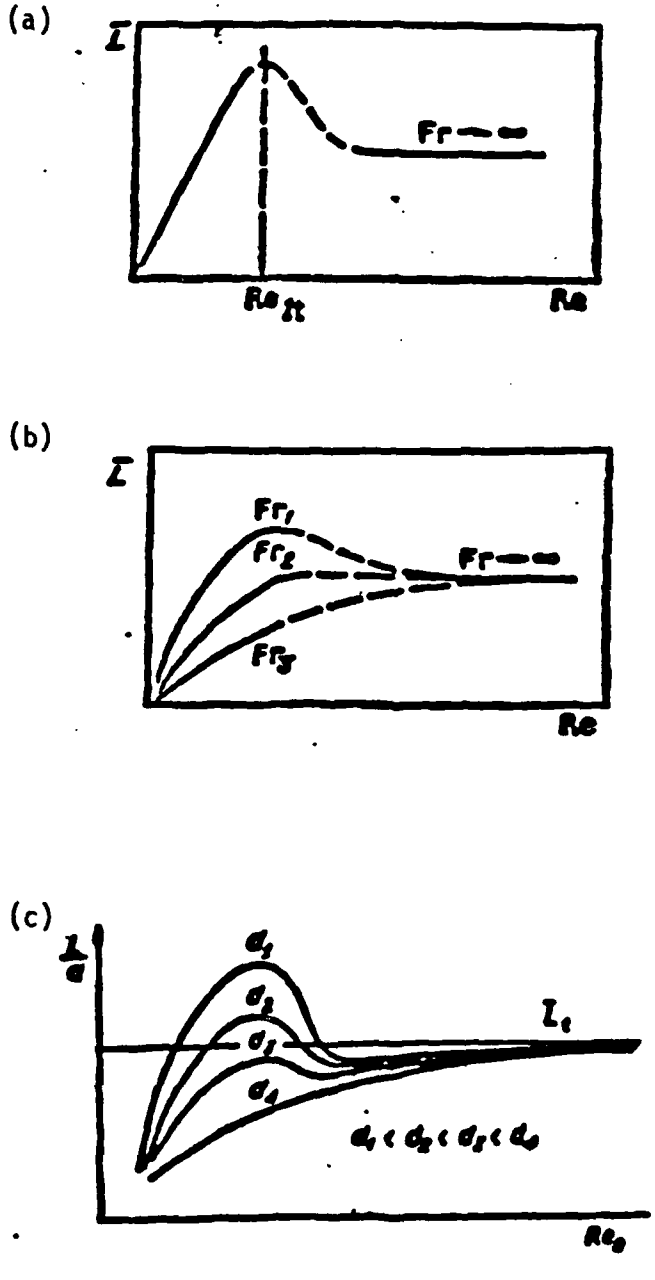

Figure 13 .

COMPARISON OF OUR HYDROGEN DATA FOR VARIOUS JET DIAMETERS

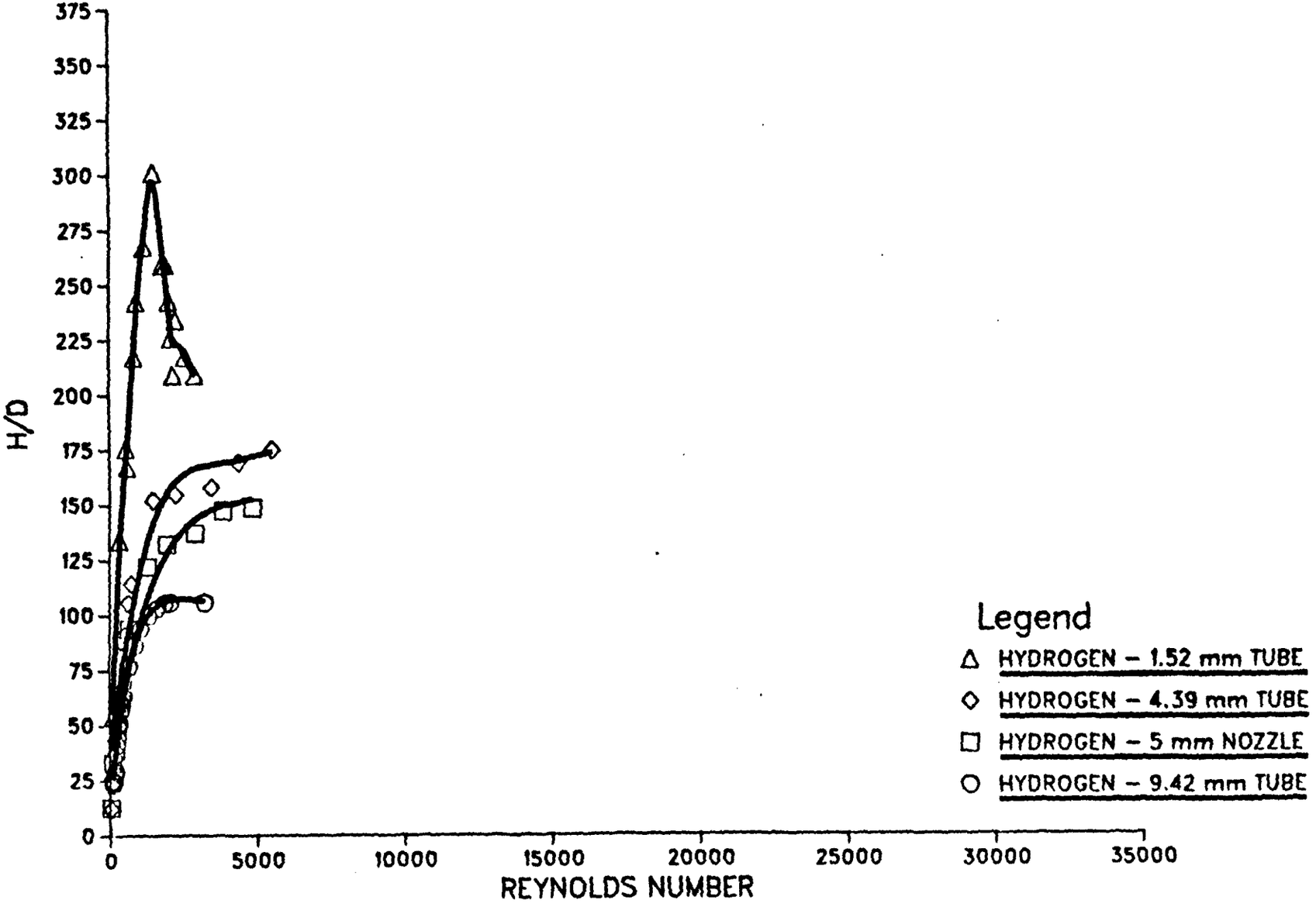

Figure 14a

COMPARISON OF OUR METHANE DATA FOR VARIOUS JET DIAMETERS

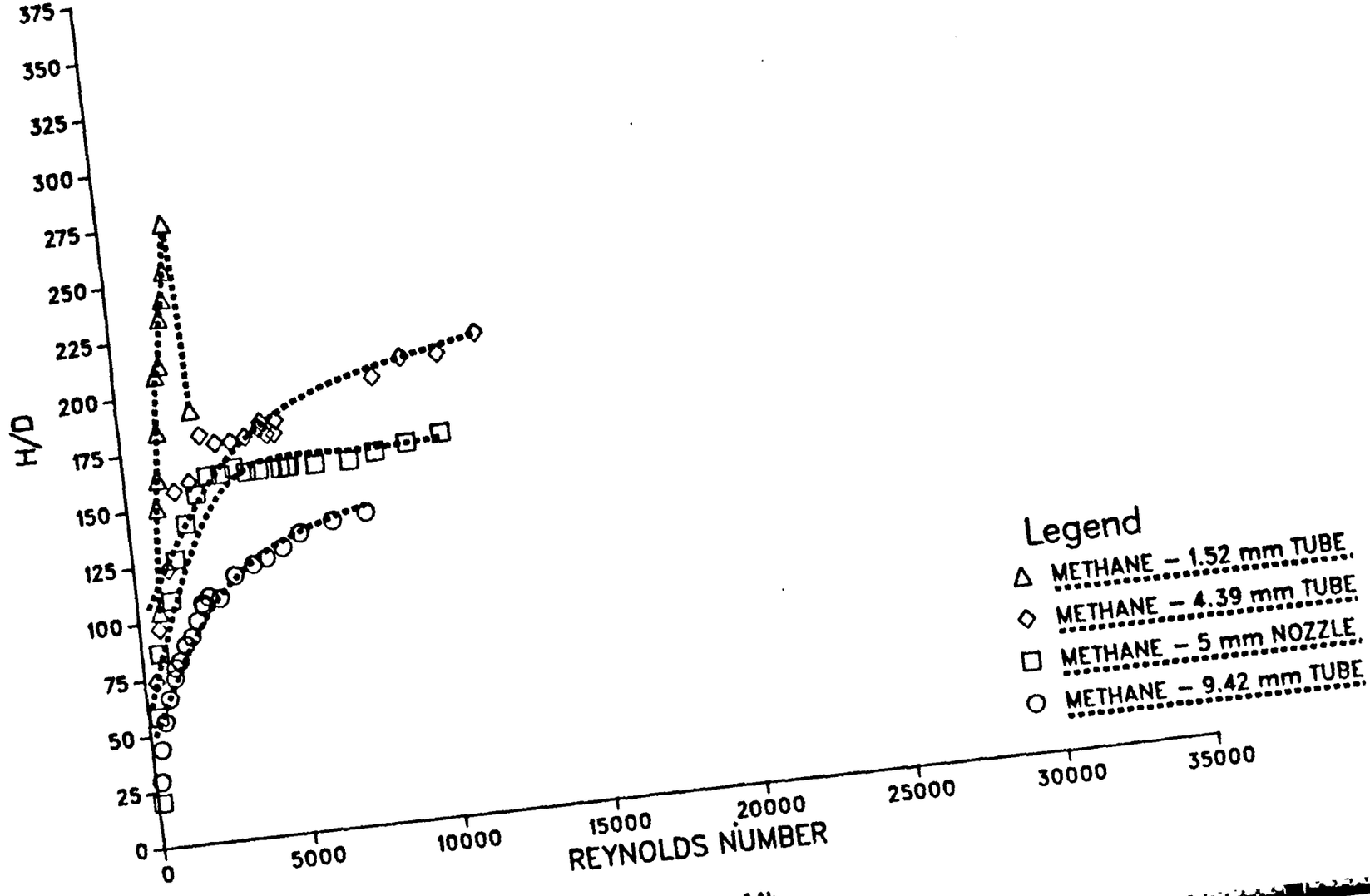

Figure 14b

COMPARISON OF OUR PROPANE DATA FOR VARIOUS JET DIAMETERS

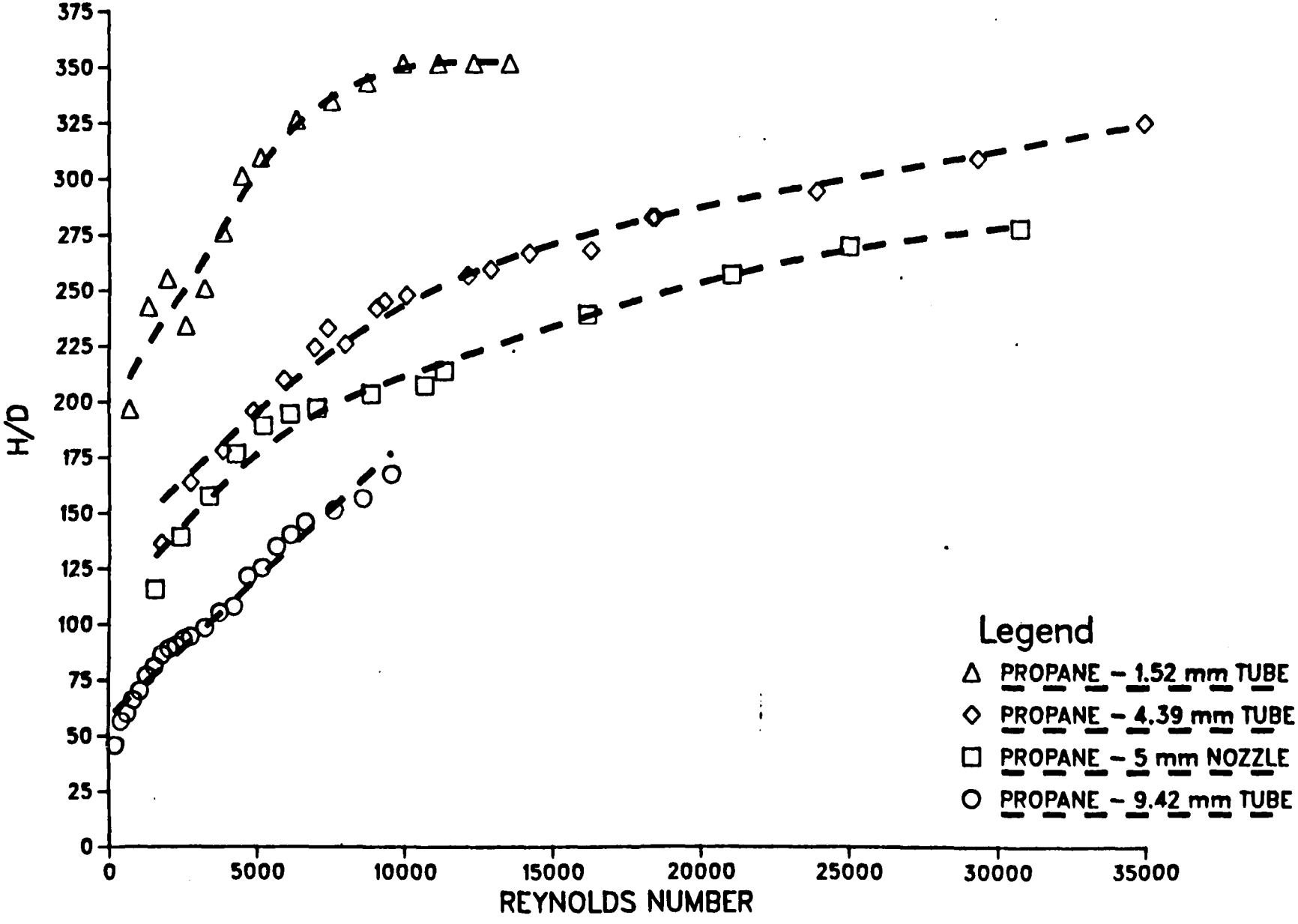

Figure 14c

COMPARISON OF OUR DATA FOR VARIOUS FUELS AND DIAMETERS

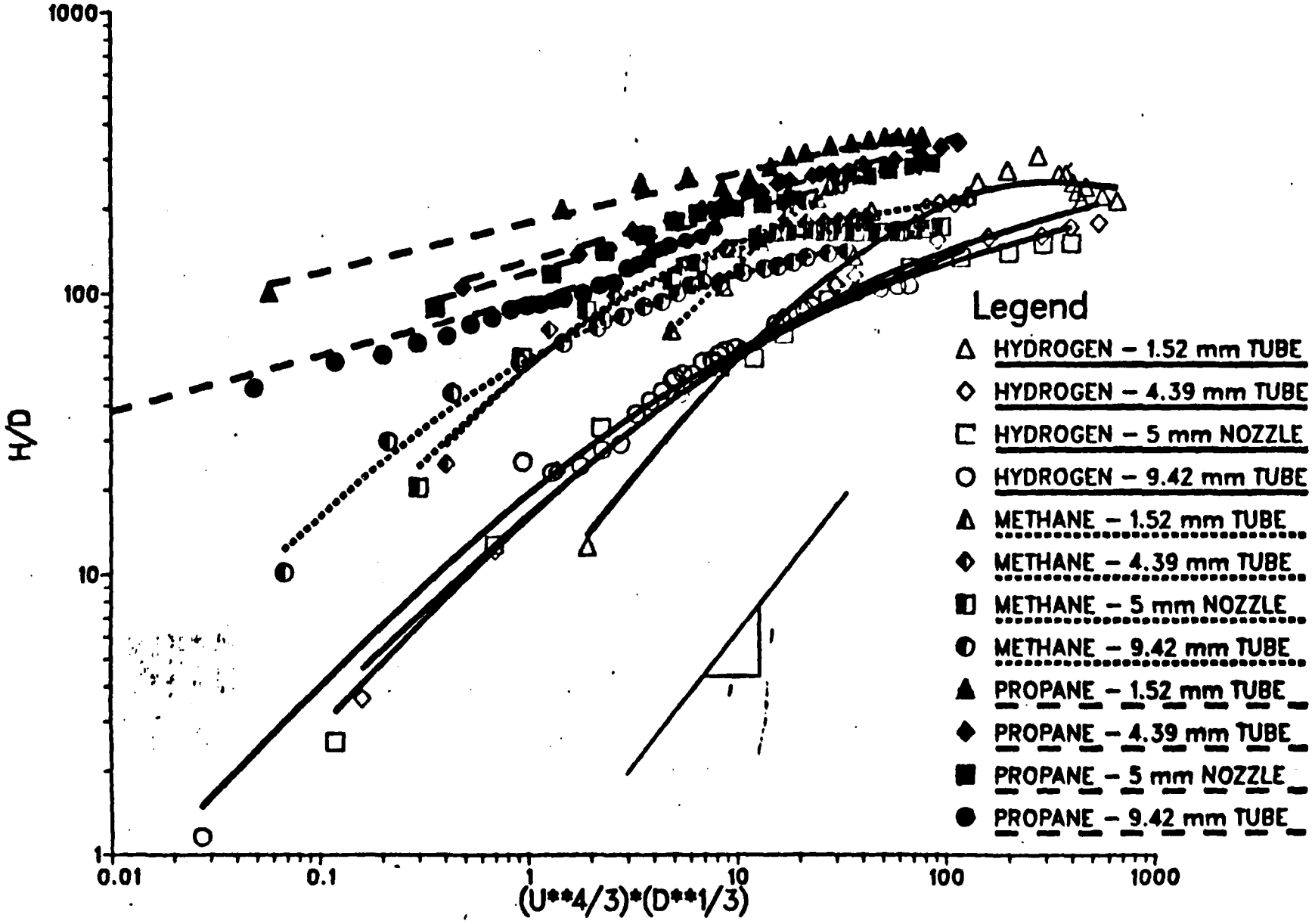

Figure 15

COMPARISON OF OUR DATA FOR VARIOUS FUELS AND DIAMETERS

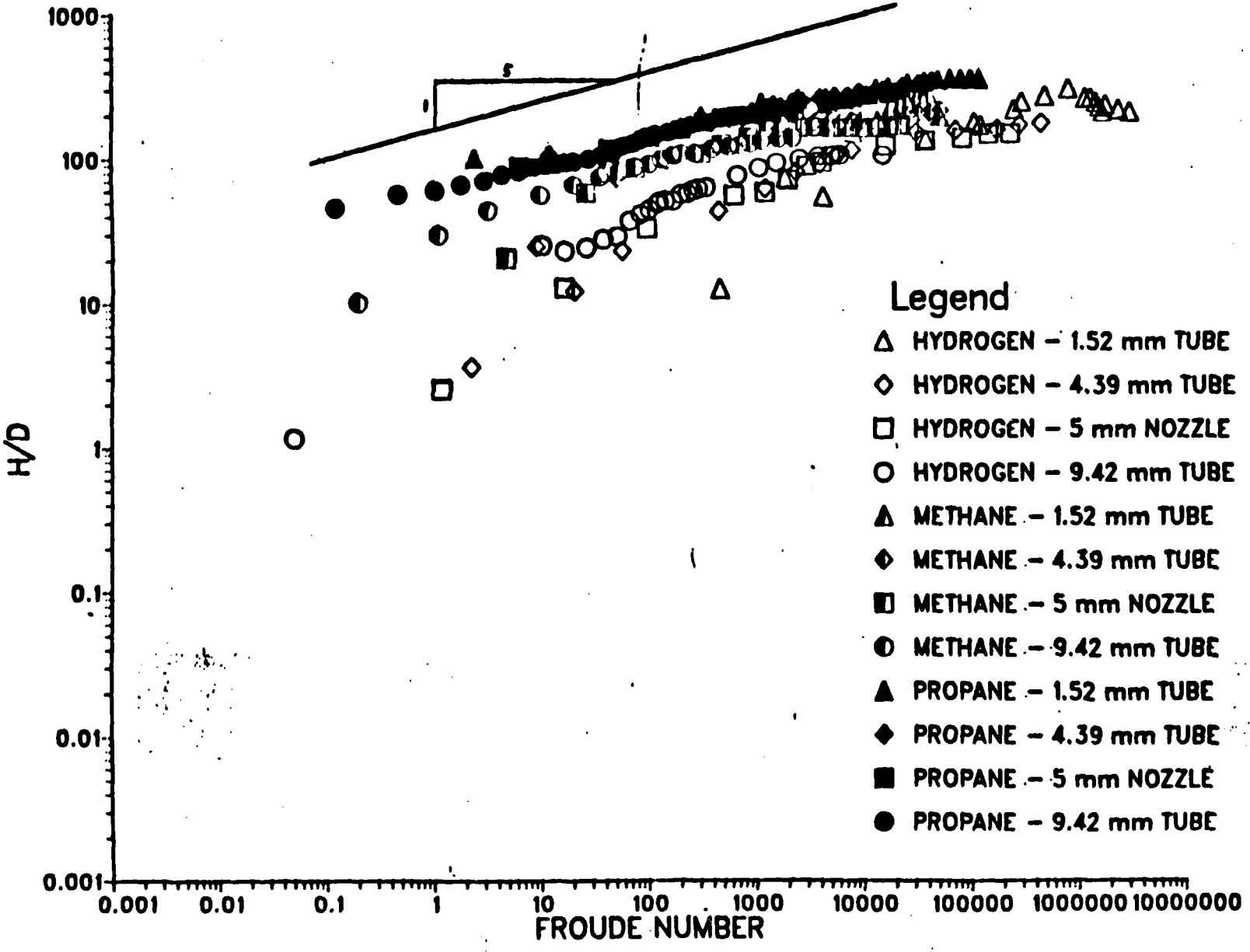

Figure 16

COMPARISON OF VARIOUS HYDROGEN DATA

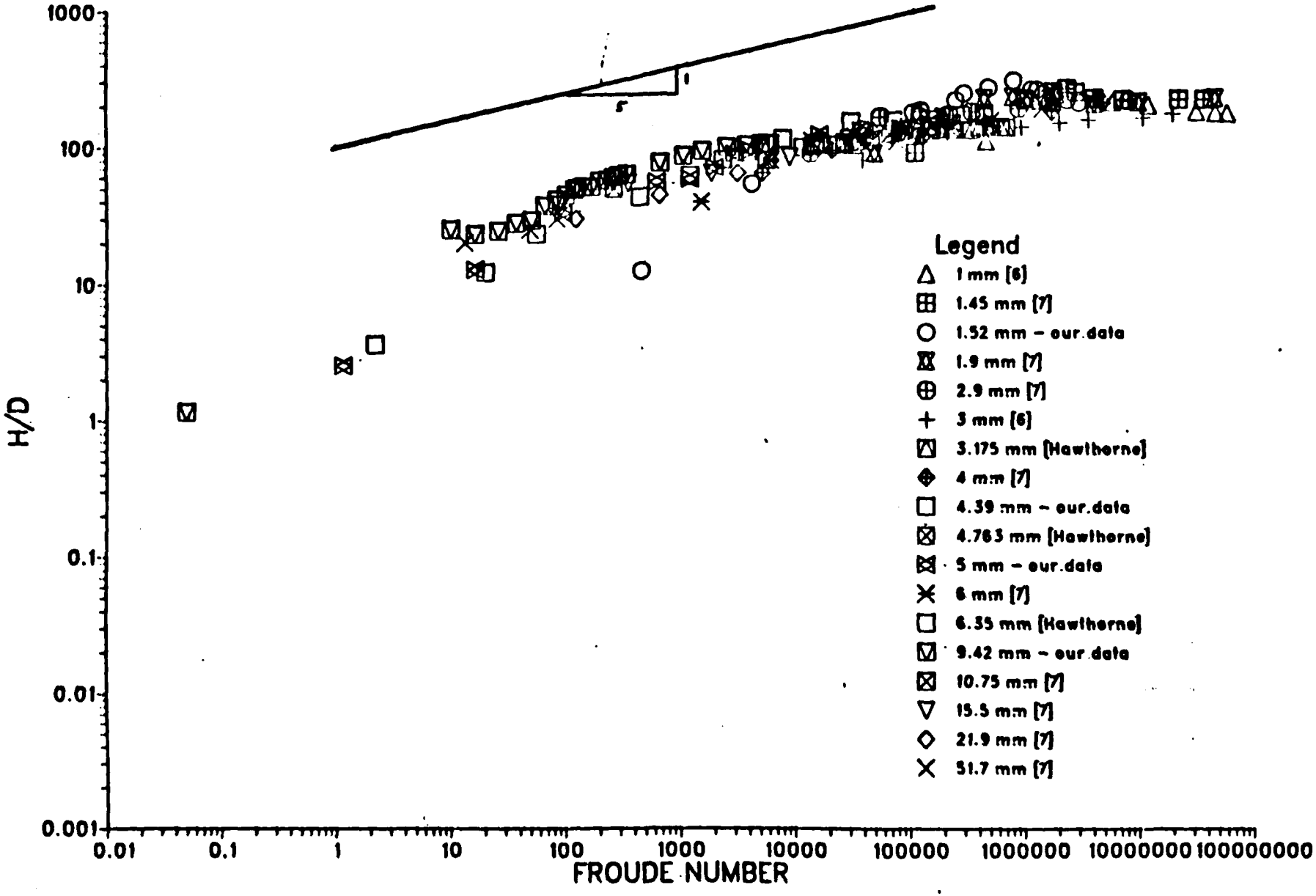

Figure 17

COMPARISON OF VARIOUS PROPANE DATA

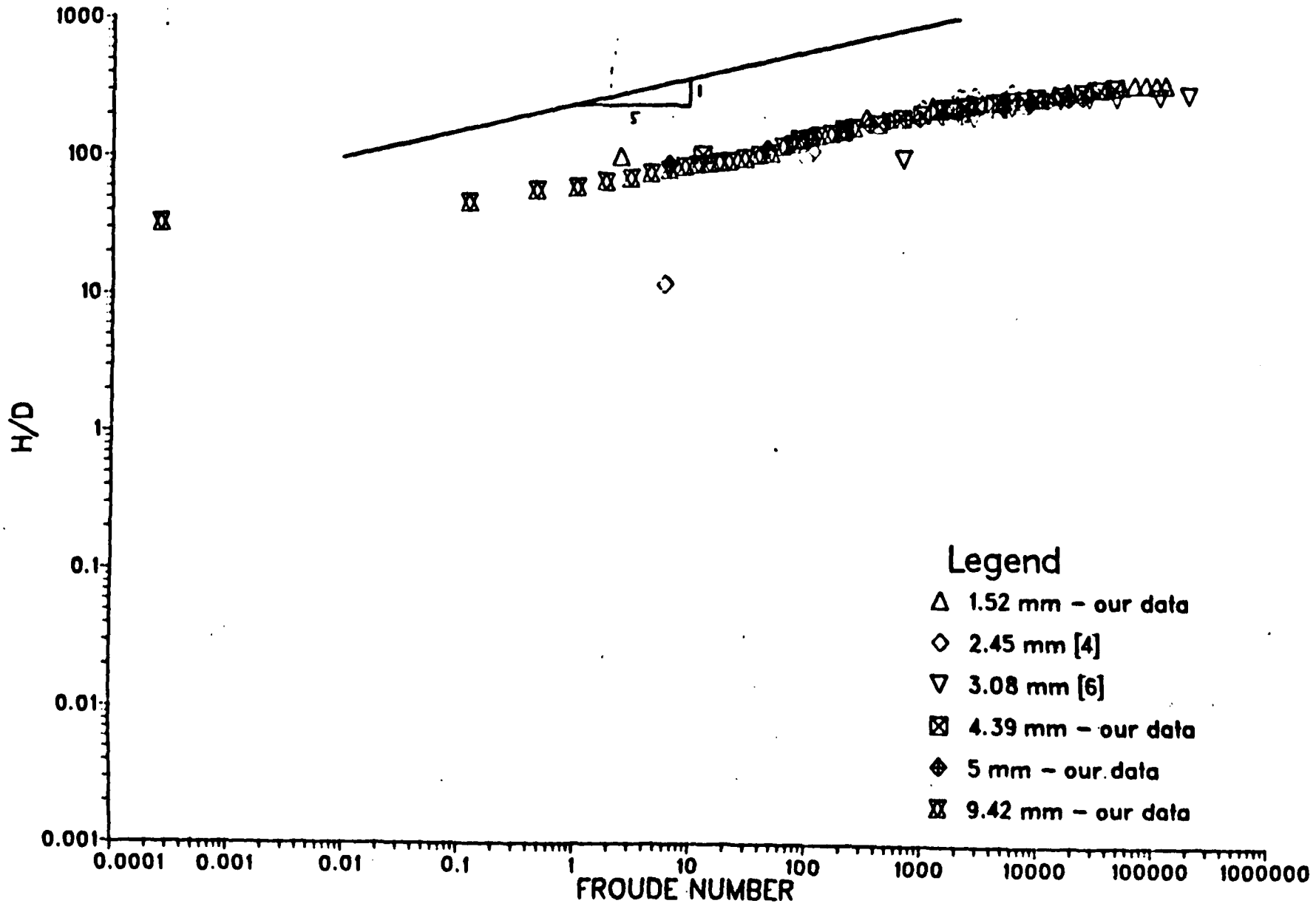

Figure 18

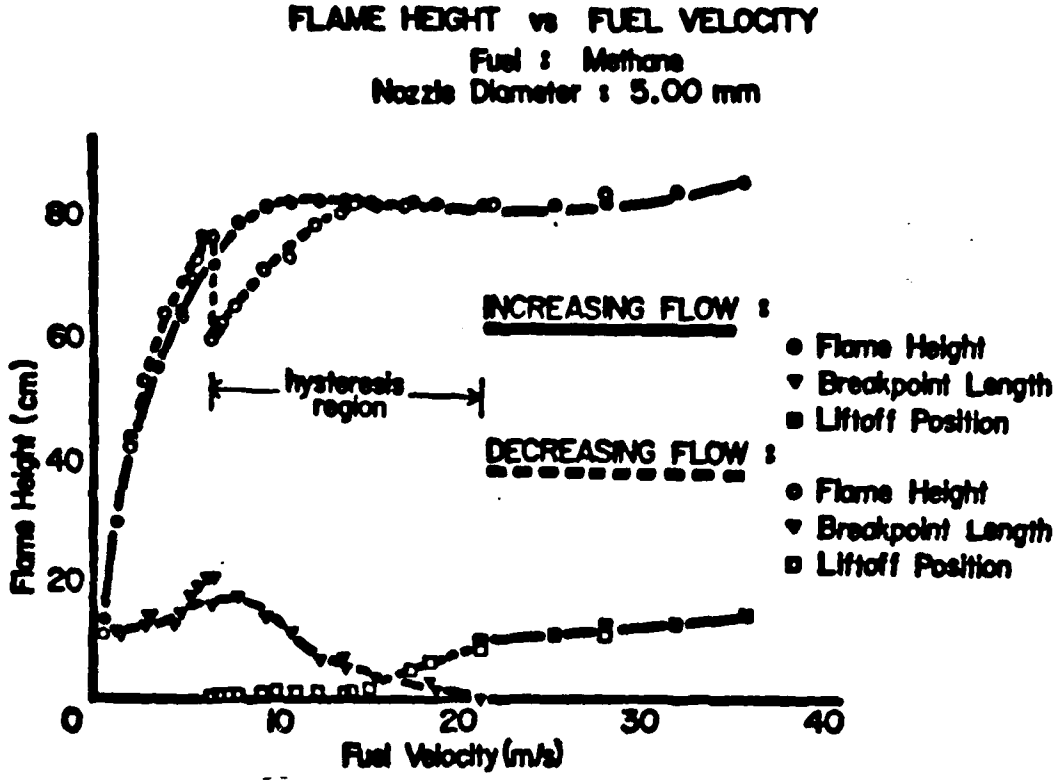

Figure 19

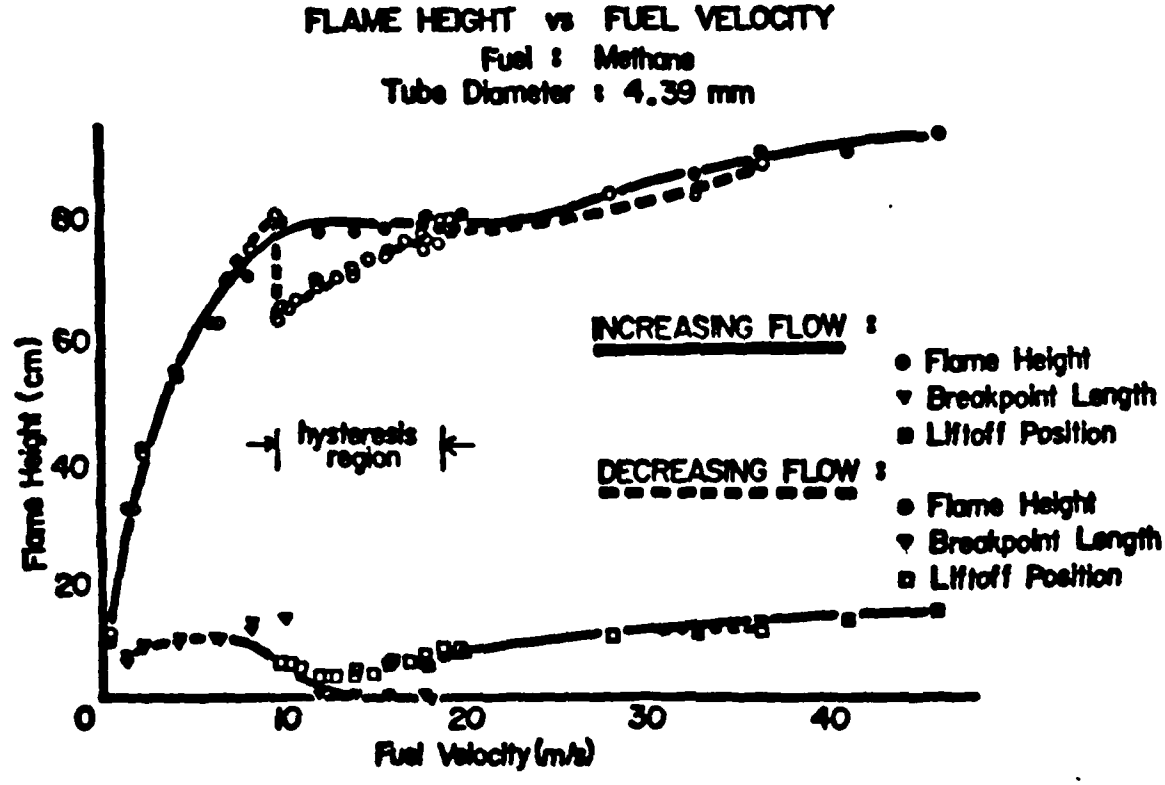

Figure 20

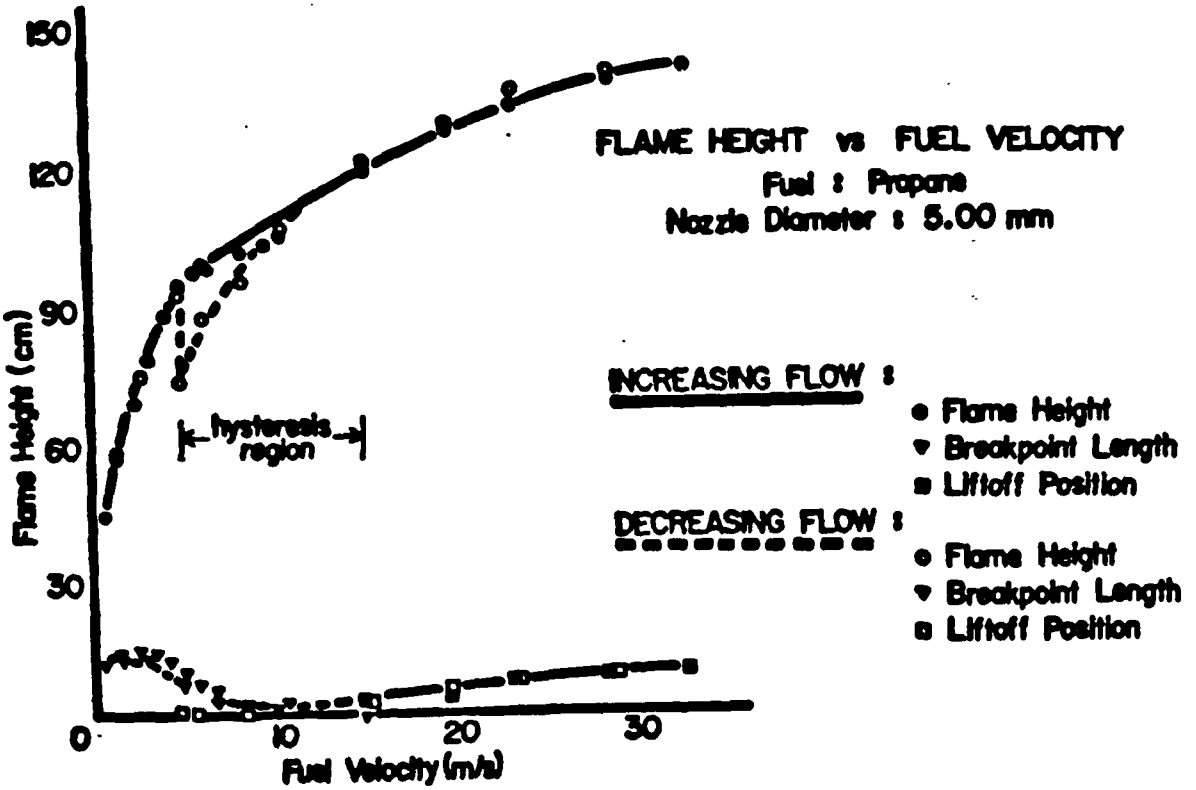

Figure 21

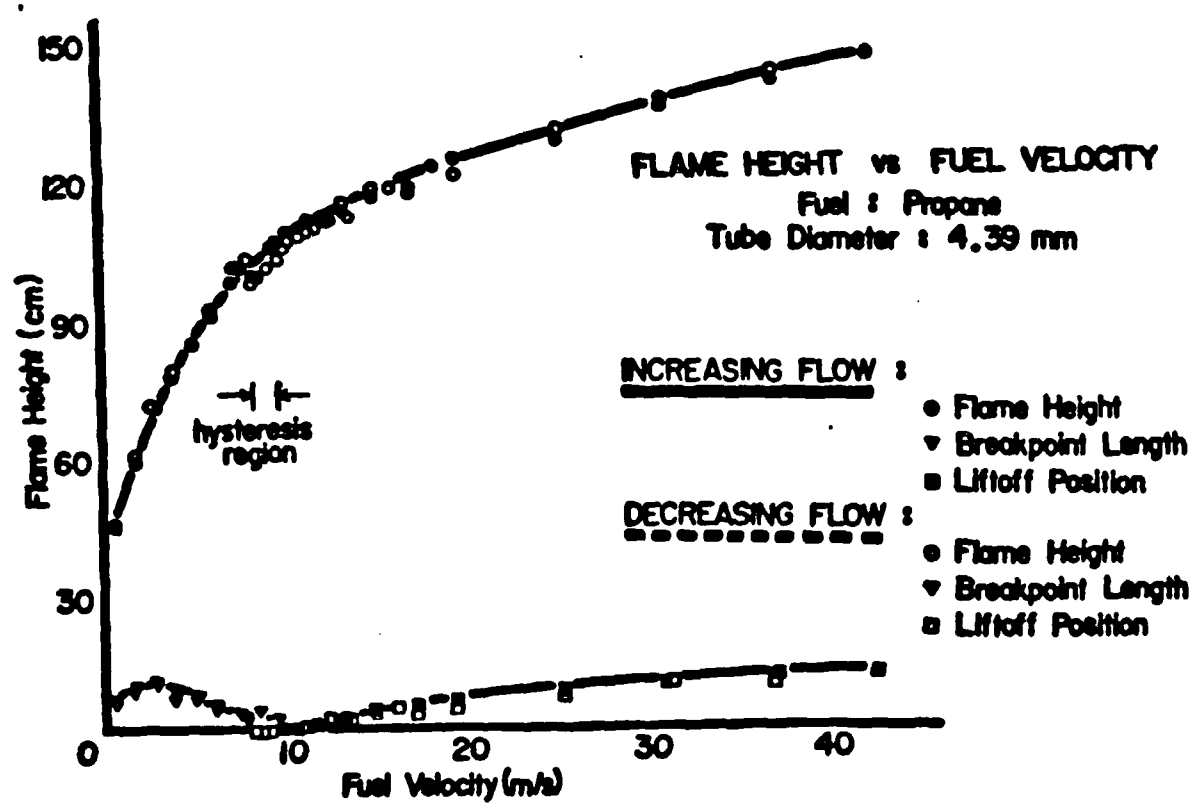

Figure 22

attached lifted

attached lifted

PROPANE
fuel velocity : 11.5 m/s
Reynolds Number : 12,487

Figure 23

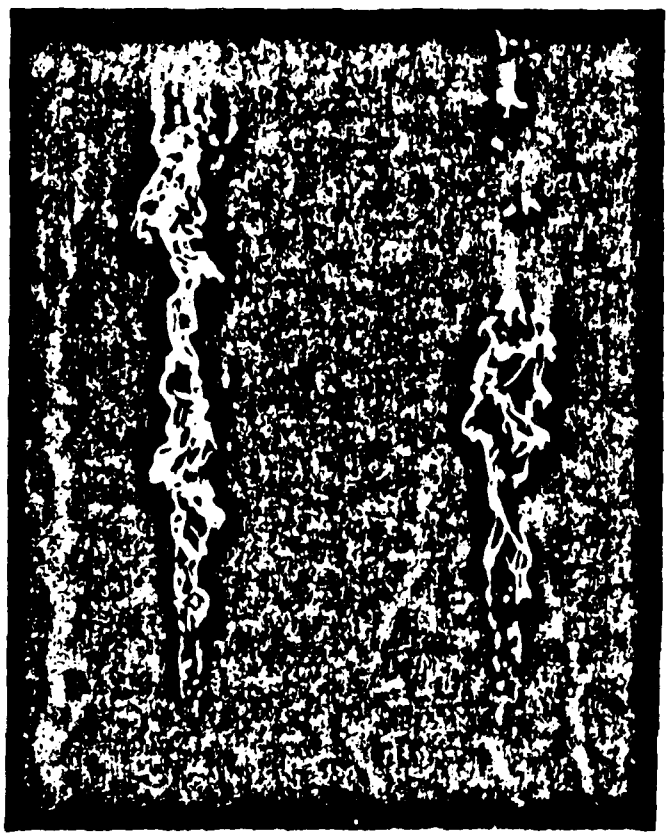

attached lifted

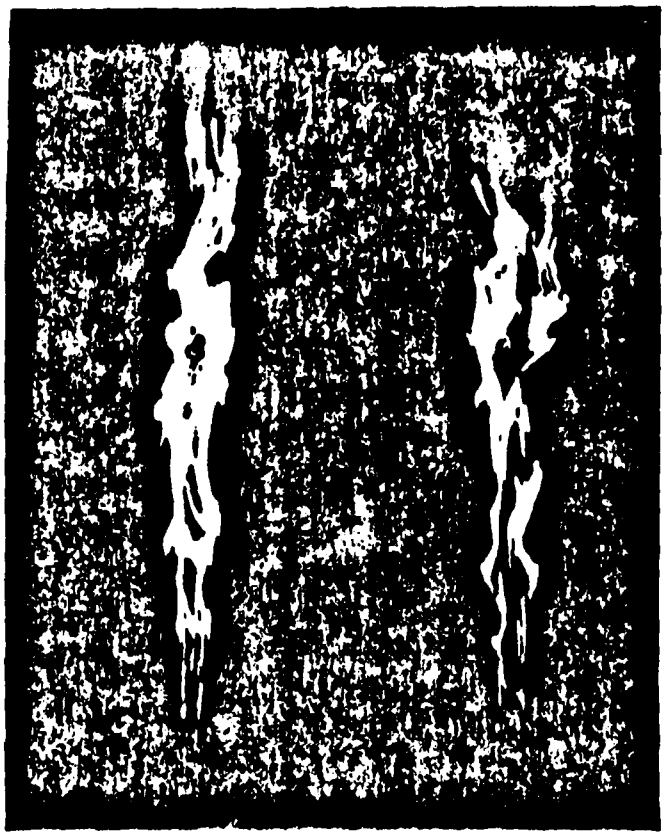

attached lifted

PROPANE
fuel velocity : 9.86 m/s
Reynolds Number : 10,676

Figure 24

attached lifted

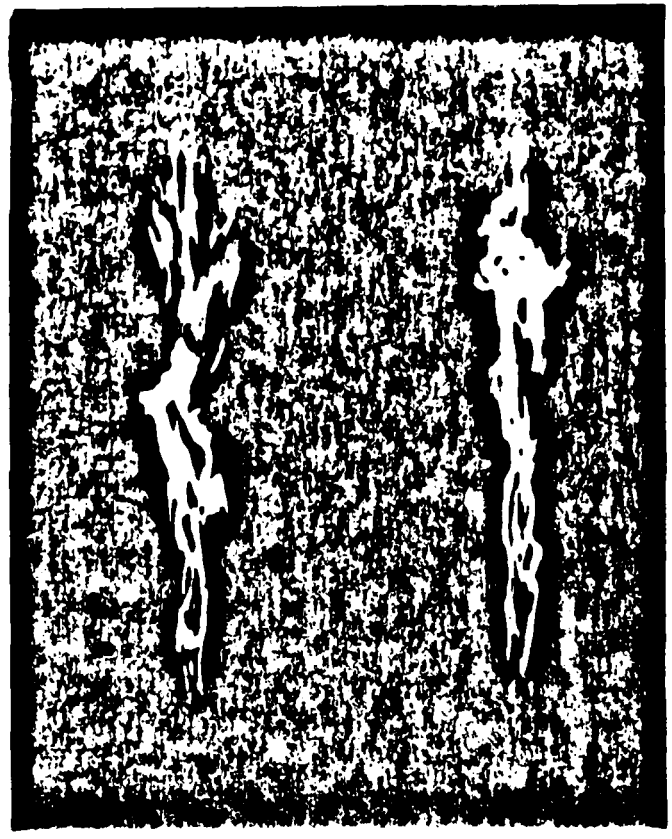

attached lifted

PROPANE
fuel velocity : 8.17 m/s
Reynolds Number : 8,853

Figure 25

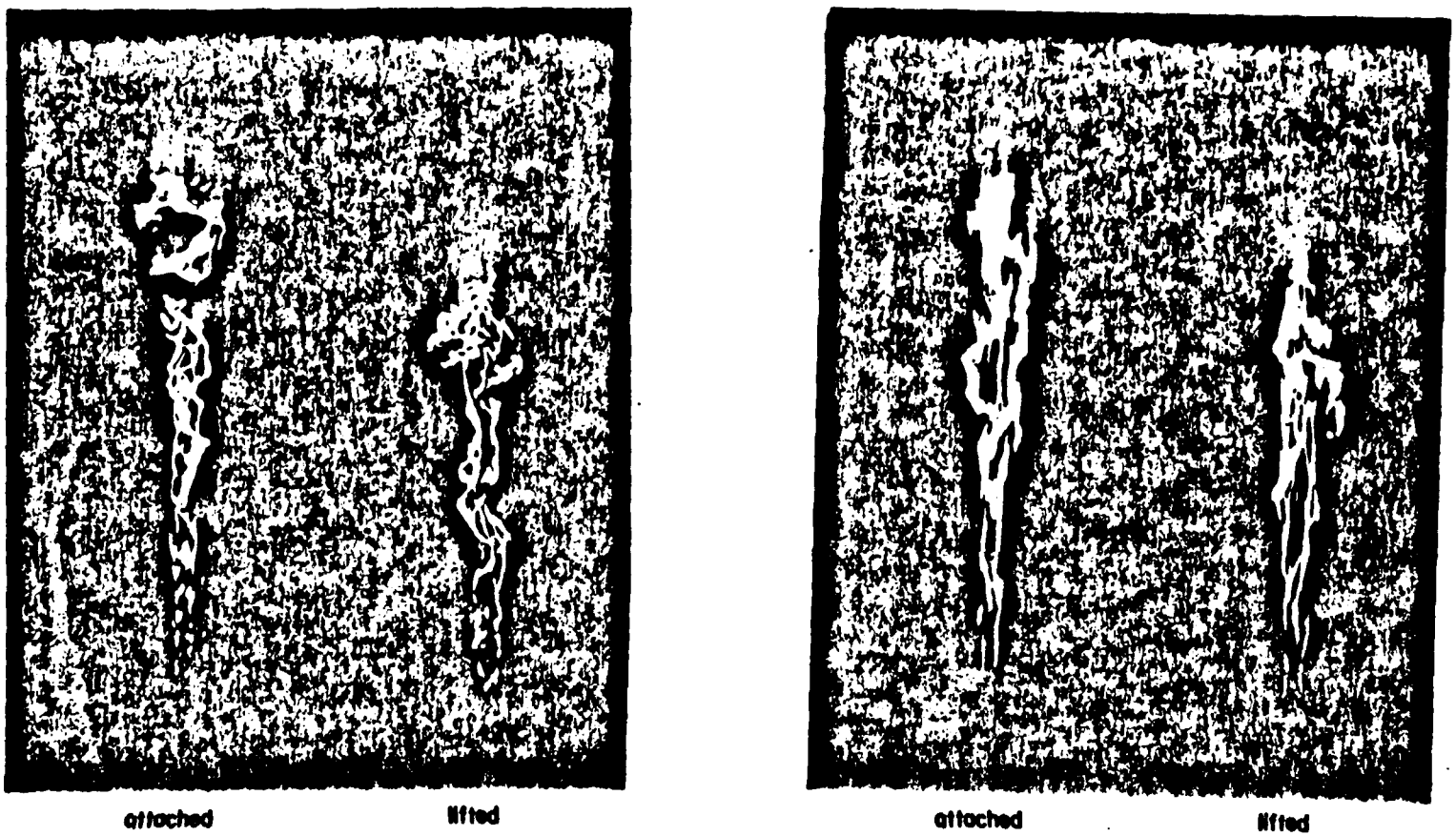

PROPANE
fuel velocity : 6.49 m/s
Reynolds Number : 7,031

Figure 26

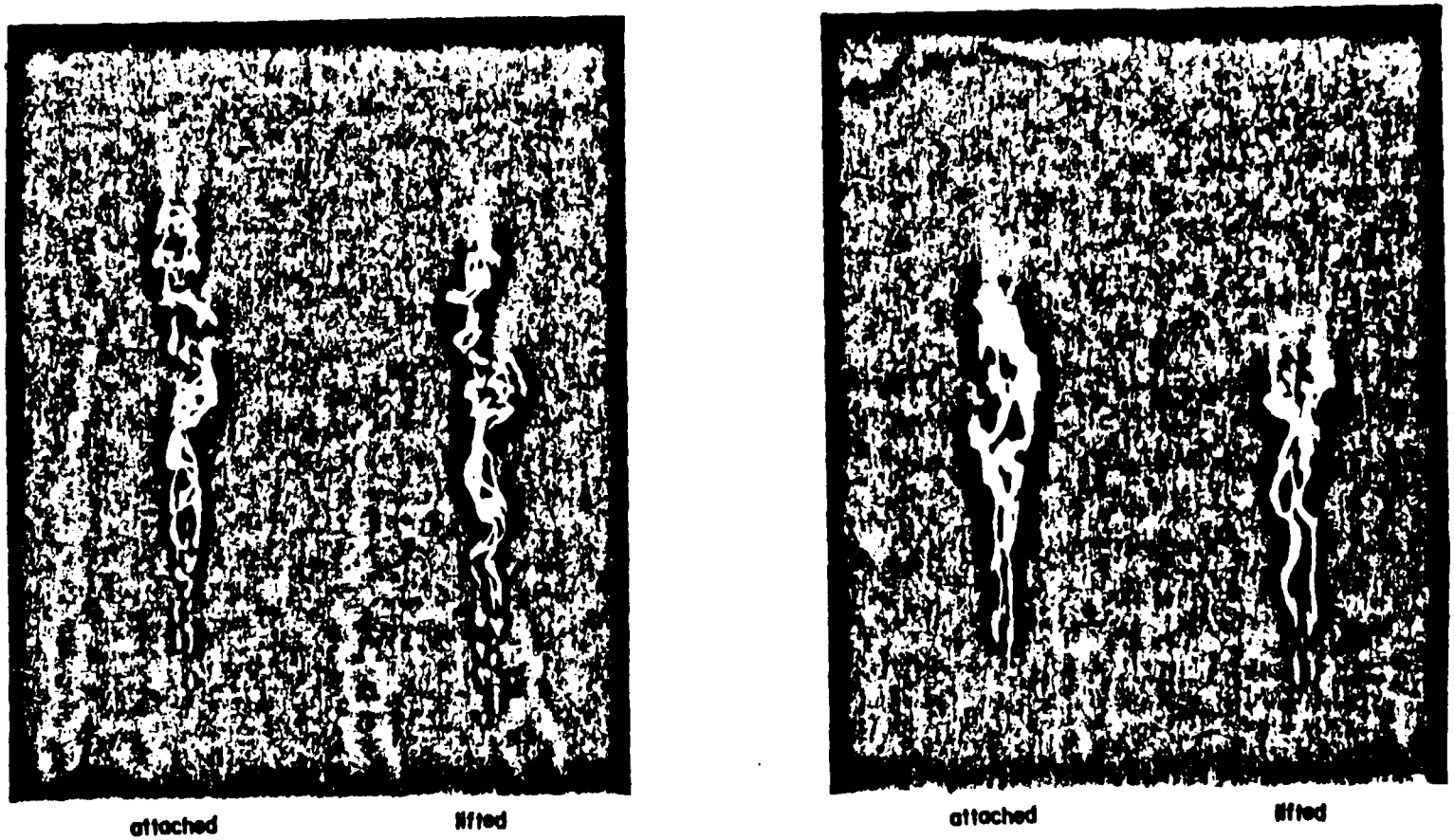

PROPANE
fuel velocity : 4.81 m/s
Reynolds Number : 5,209

Figure 27

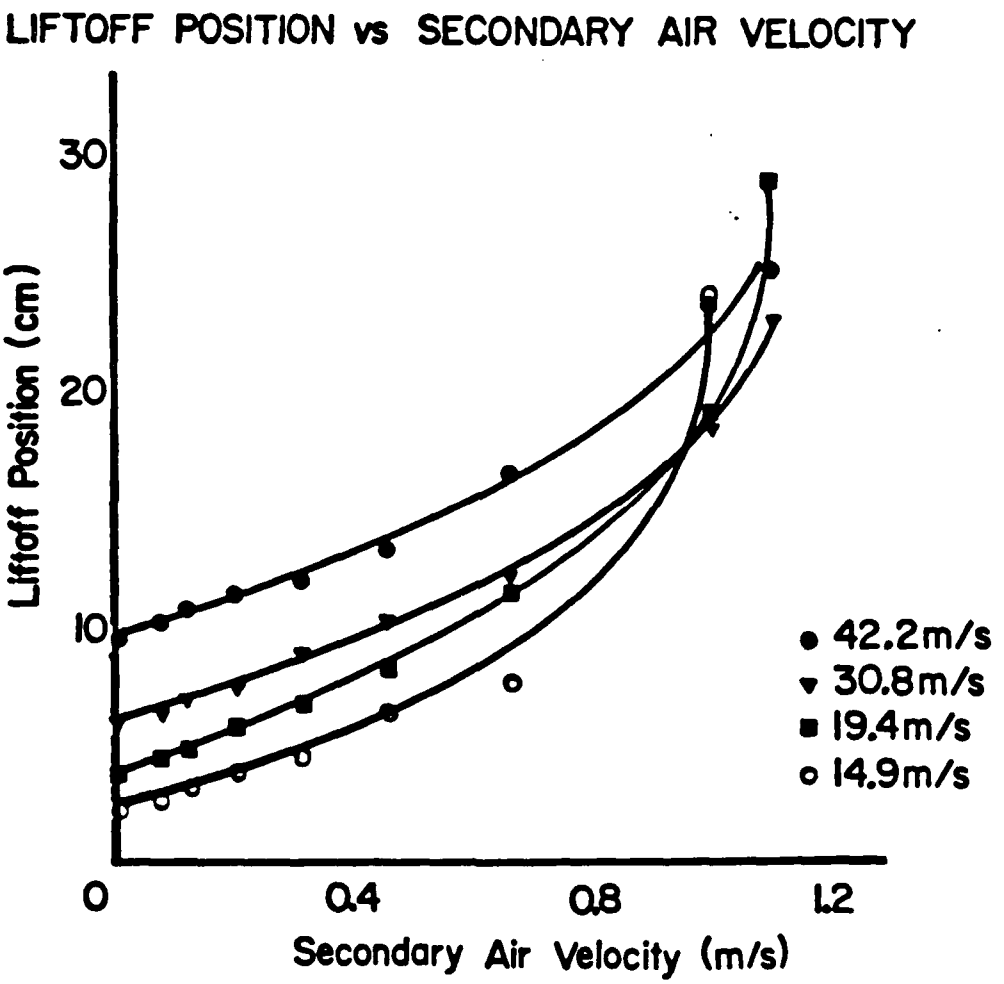
LIFTOFF POSITION vs SECONDARY AIR VELOCITY
Liftoff Position (cm)
30
20
10
0
0.4
0.8
1.2
Secondary Air Velocity (m/s)
● 42.2m/s
▼ 30.8m/s
■ 19.4m/s
○ 14.9m/s

Figure 28

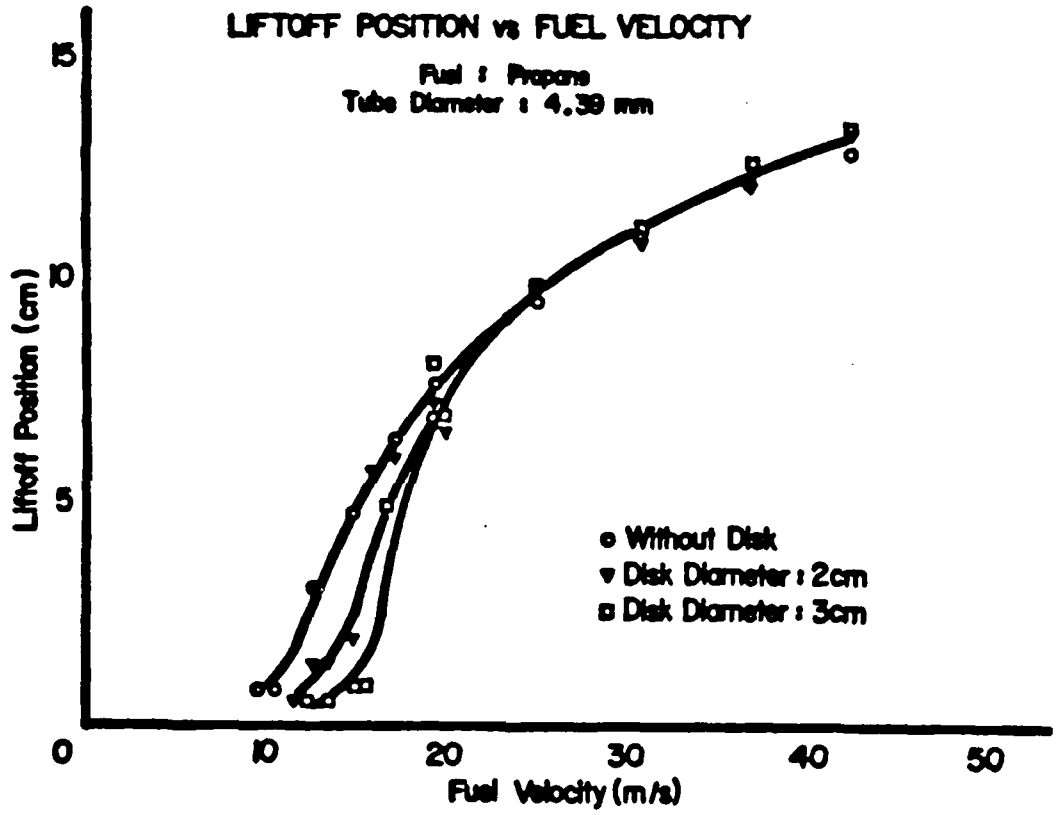
LIFTOFF POSITION vs FUEL VELOCITY
Fuel : Propane
Tube Diameter : 4.39 mm
Liftoff Position (cm)
15
10
5
0
10
20
30
40
50
Fuel Velocity (m/s)
o Without Disk
▼ Disk Diameter : 2cm
□ Disk Diameter : 3cm

Figure 29

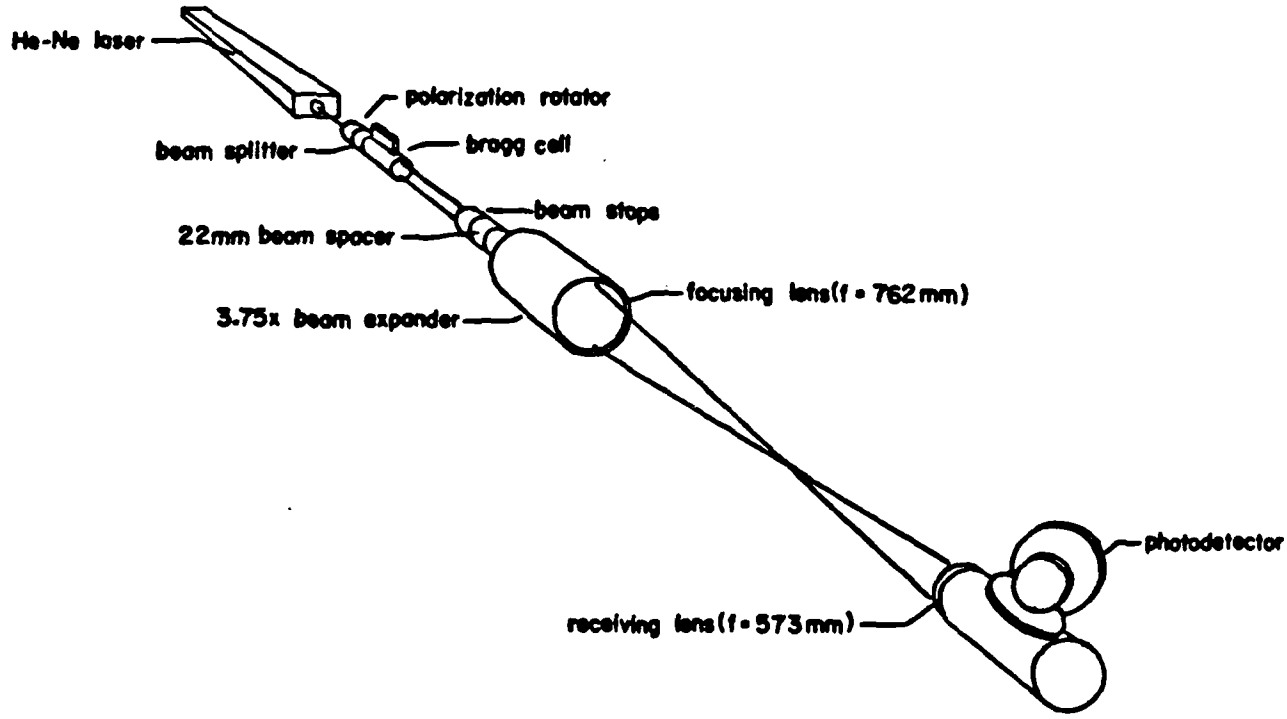

OPTICAL ARRANGEMENT for LASER ANEMOMETRY

Figure 30

LIFTED and ATTACHED PROPANE FLAME

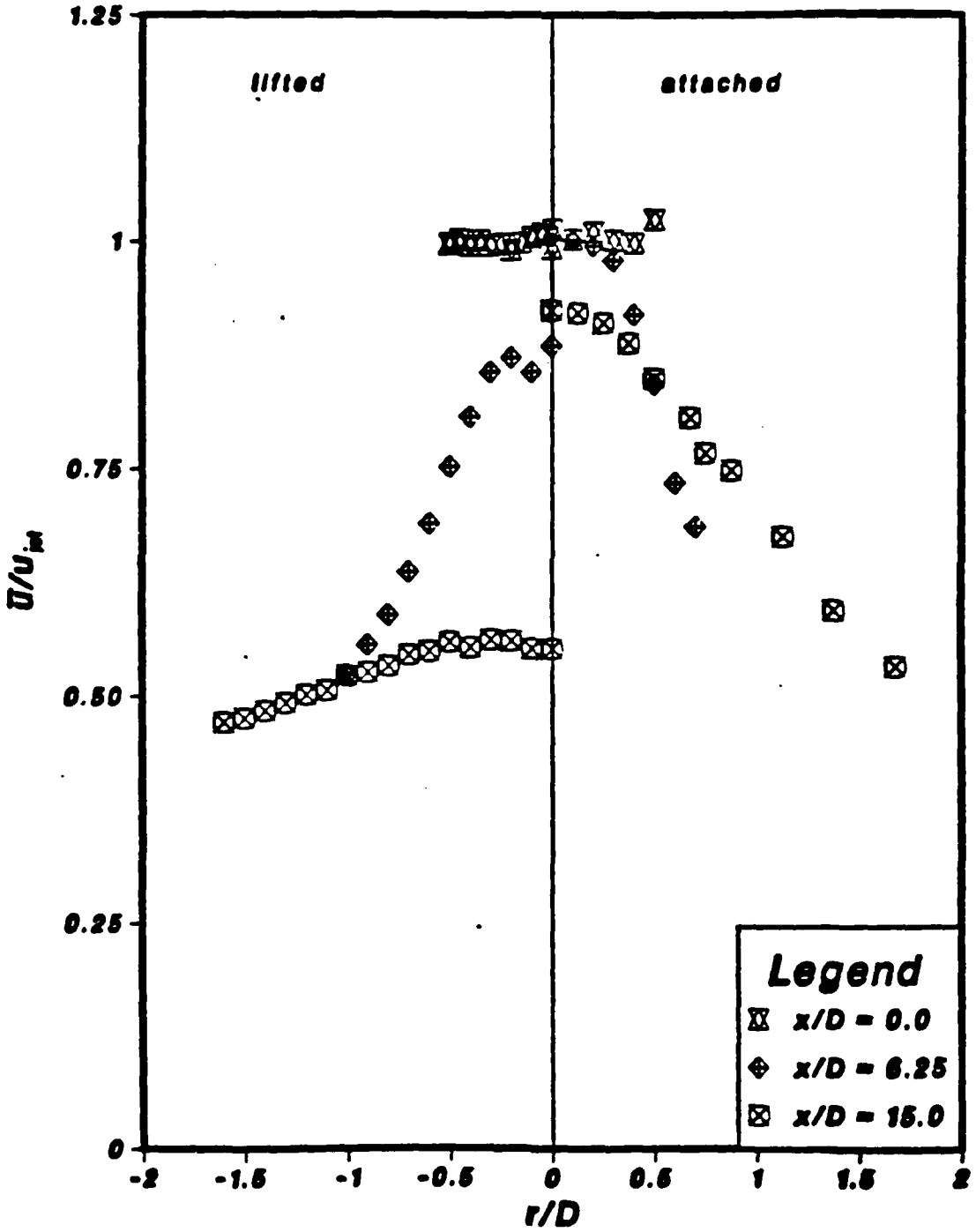

Figure 31

LIFTED and ATTACHED PROPANE FLAME

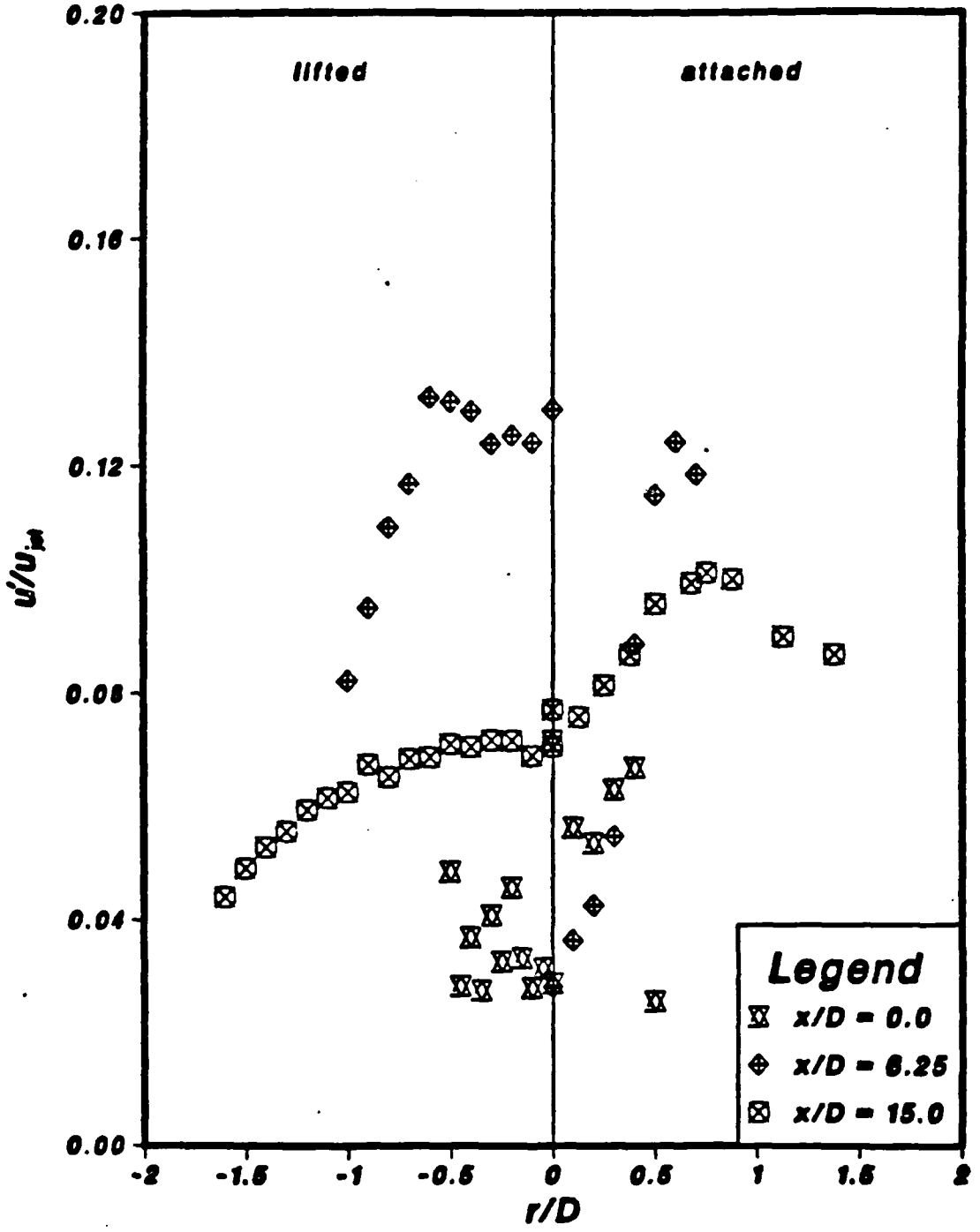

Figure 32

LIFTED and ATTACHED PROPANE FLAME

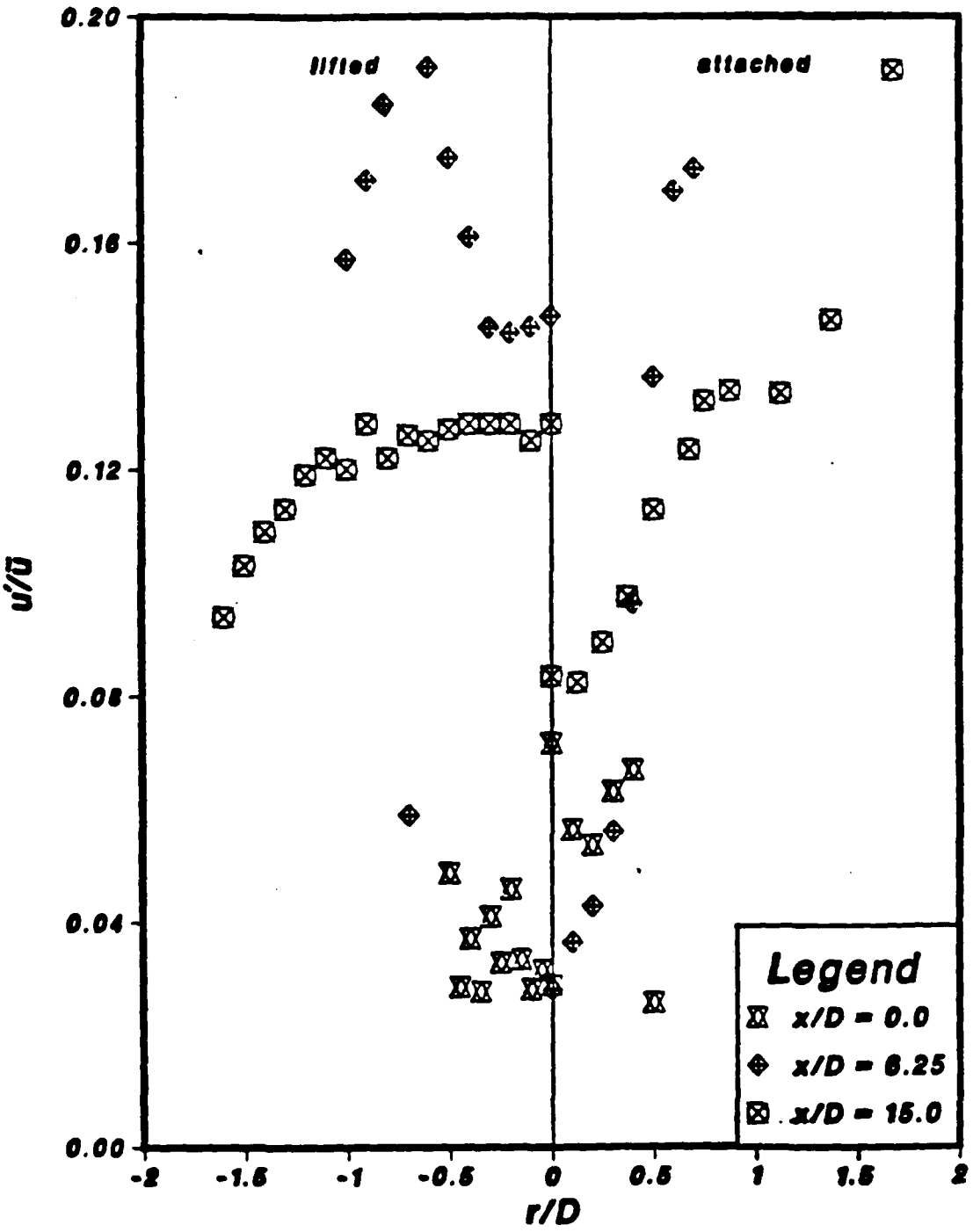

Figure 33

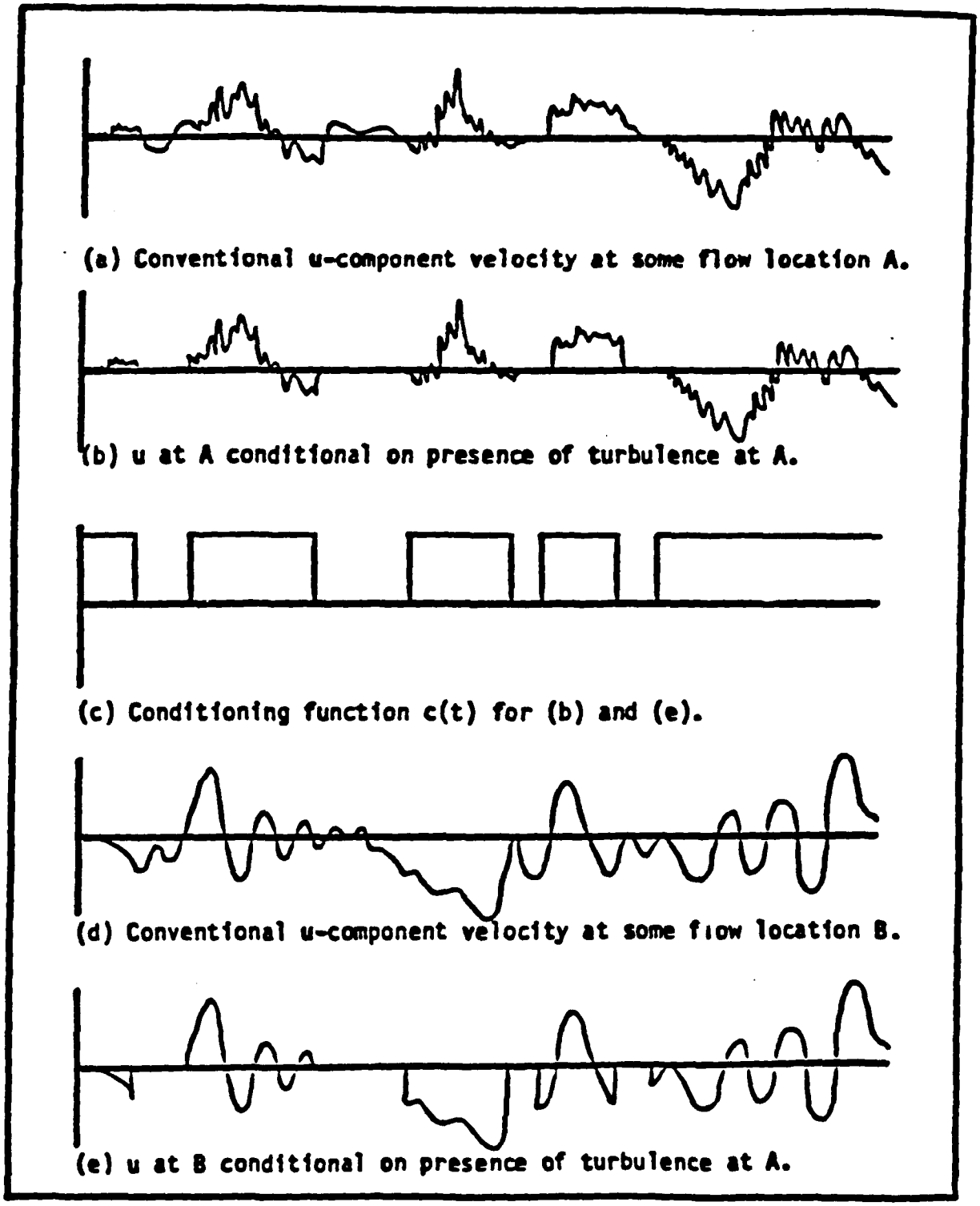

Conditional sampling of velocity data from two flow locations.

Figure 34

****

LDV - EXPERIMENT RESULTS

I. Measurement Volume location : X = 0.000 in
Y = 0.000 in
Z = 0.000 in

II. Mean Velocity of all data records :
U - component ... 12.786 M/SEC
V - component ... 0.000 M/SEC
RMS of fluctuating velocity :
U - component ... 0.365 M/SEC
V - component ... 0.000 M/SEC
Maximum Velocity :
U - component ... 13.421 M/SEC
V - component ... 0.000 M/SEC
Minimum Velocity :
U - component ... 8.921 M/SEC
V - component ... 0.000 M/SEC

III. Data Collected ... 19-OCT-57 10:35:28
Data Processed ... 27-OCT-84 11:00:41
5120 Velocity data-points taken
Frequency shift on SP0 ... 0.000 MHZ
Frequency shift on SP1 ... 0.000 MHZ
Random mode
Single velocity-component system
Data read from file DD11.DAT on 27-OCT-84 11:01:23

****

DD11B.PIC

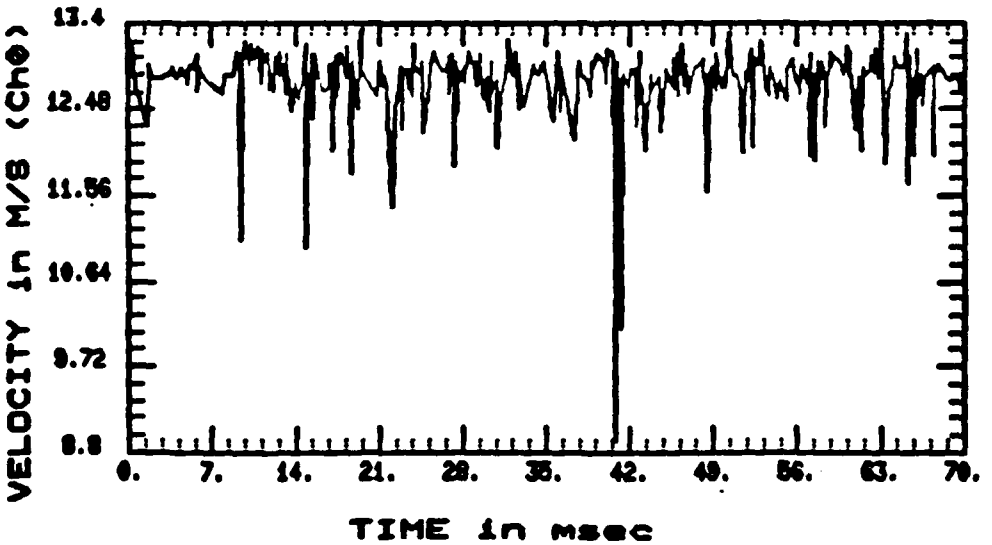

Figure 35

LDV - EXPERIMENT RESULTS

I. Measurement Volume location : X = 0.000 in
Y = -0.080 in
Z = 0.000 in

II. Mean Velocity of all data records :
U - component ... 12.560 M/SEC
V - component ... 0.000 M/SEC
RMS of fluctuating velocity :
U - component ... 0.468 M/SEC
V - component ... 0.000 M/SEC
Maximum Velocity :
U - component ... 13.330 M/SEC
V - component ... 0.000 M/SEC
Minimum Velocity :
U - component ... 8.369 M/SEC
V - component ... 0.000 M/SEC

III. Data Collected ... 19-OCT-57 10:43:55
Data Processed ... 27-OCT-84 11:49:22
5120 Velocity data-points taken
Frequency shift on SP0 ... 0.000 MHZ
Frequency shift on SP1 ... 0.000 MHZ
Random mode
Single velocity-component system
Data read from file DD19.DAT on 27-OCT-84 11:50:08

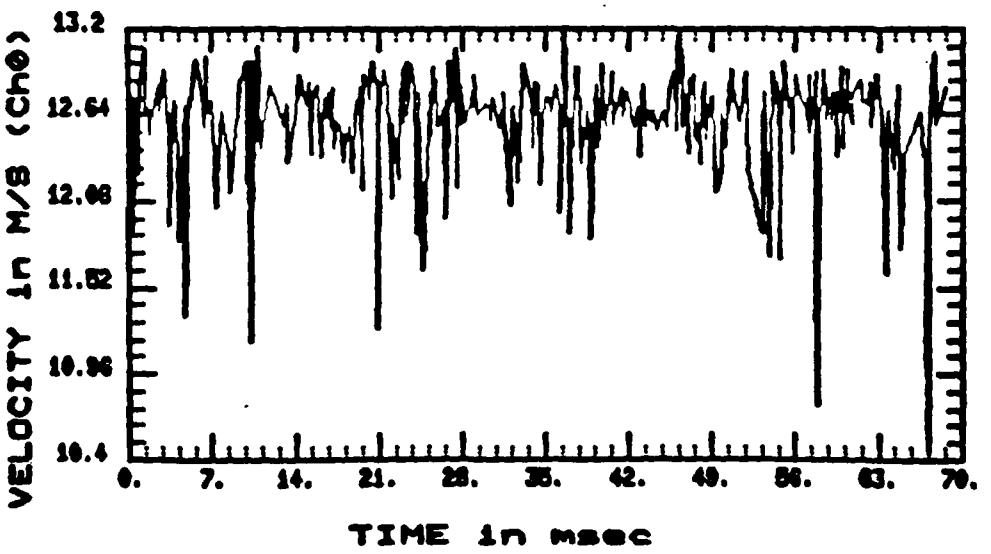

Figure 36

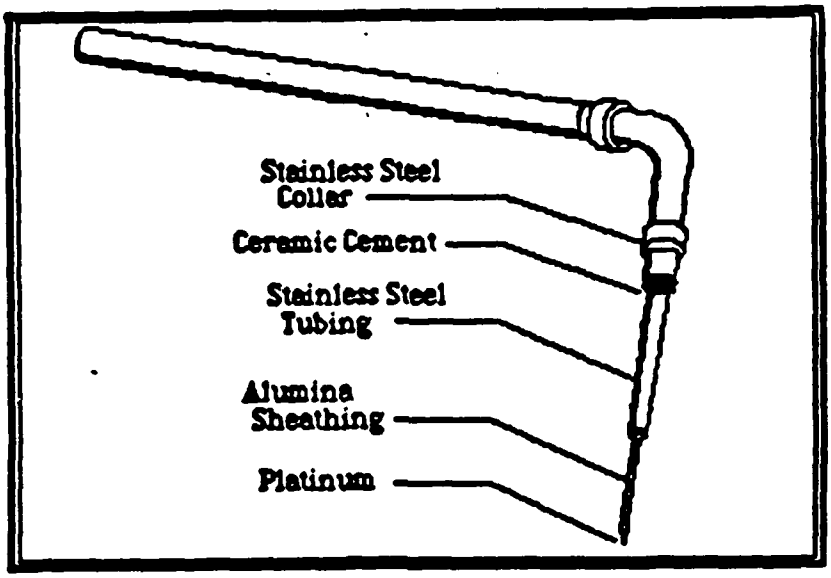

Current probe configuration

Figure 37

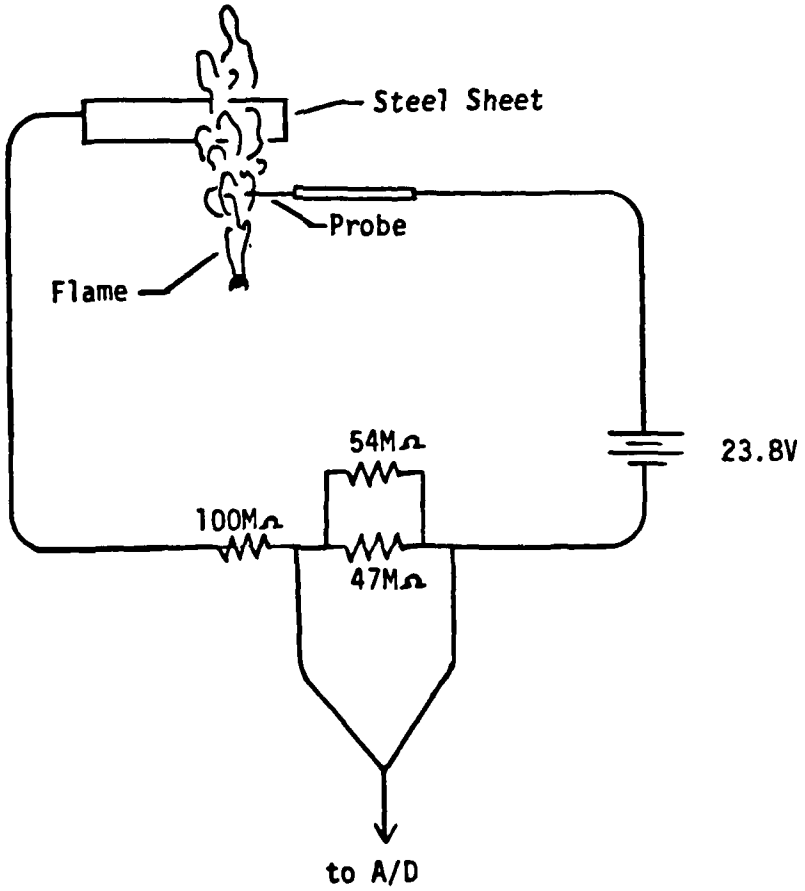

Figure 38

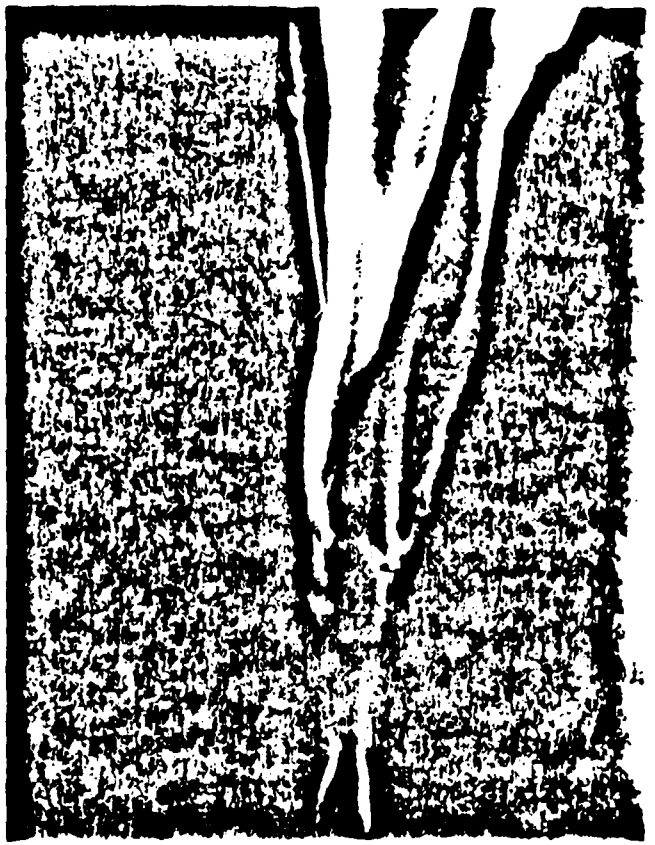

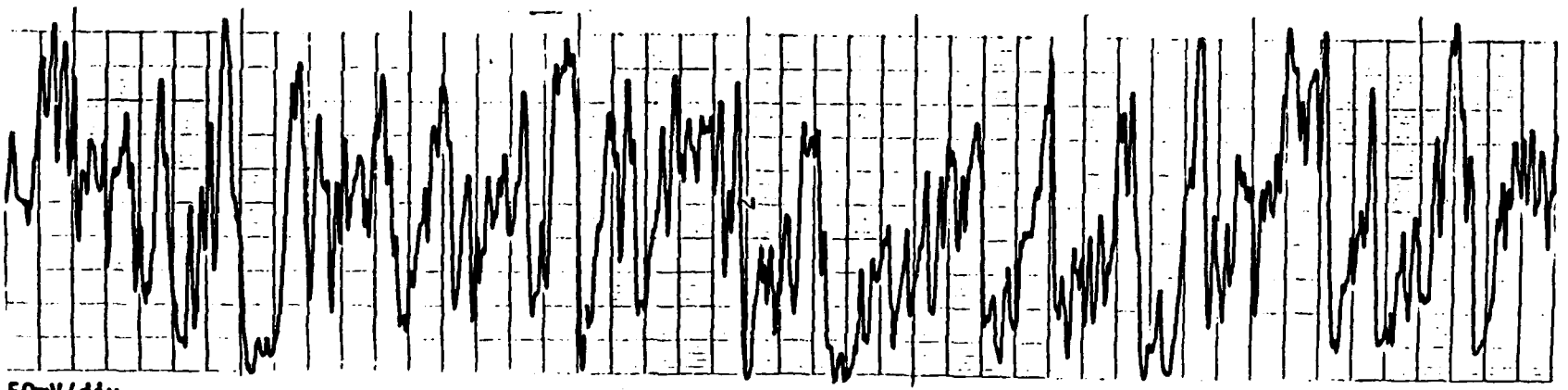

Figure 39

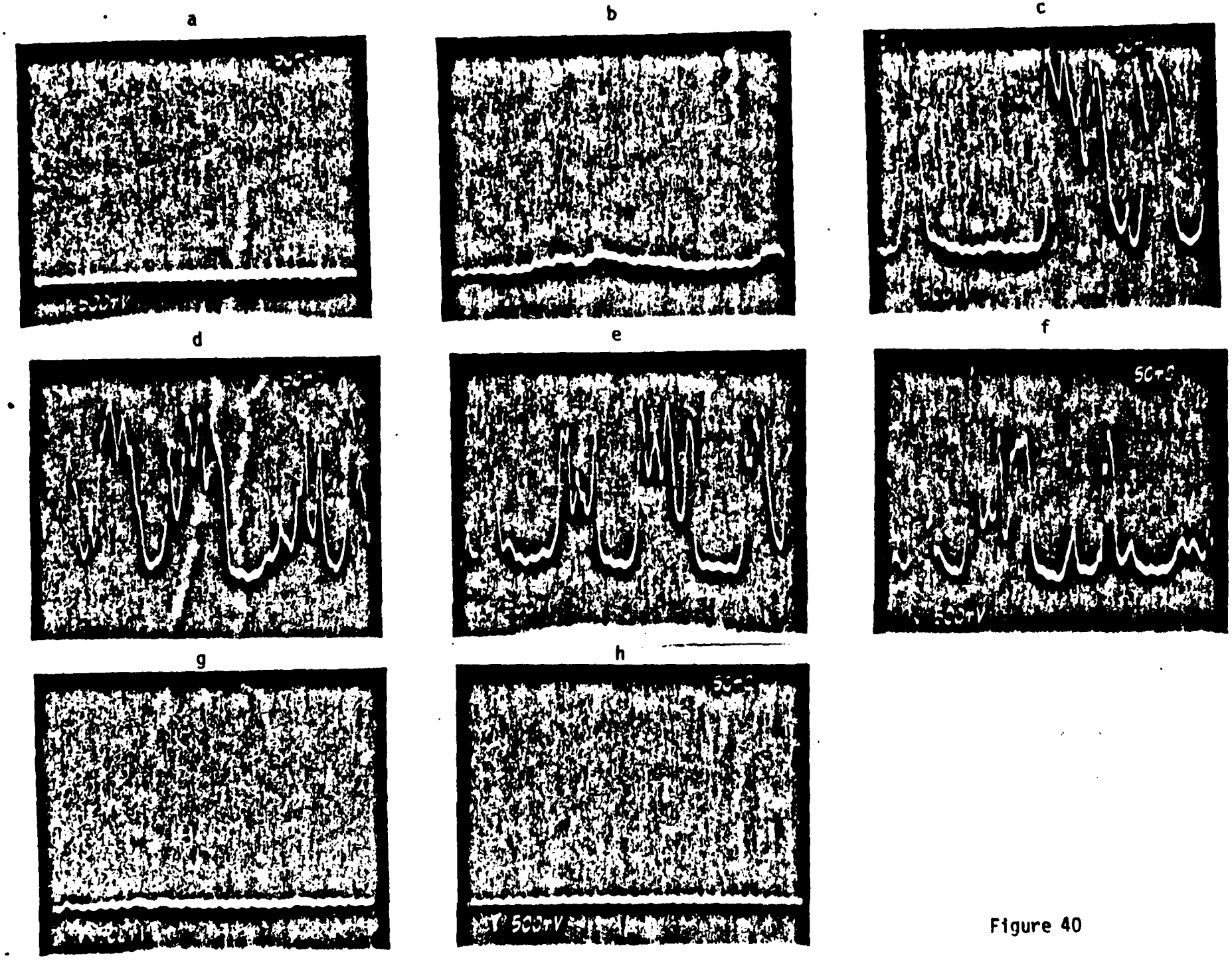

Figure 40

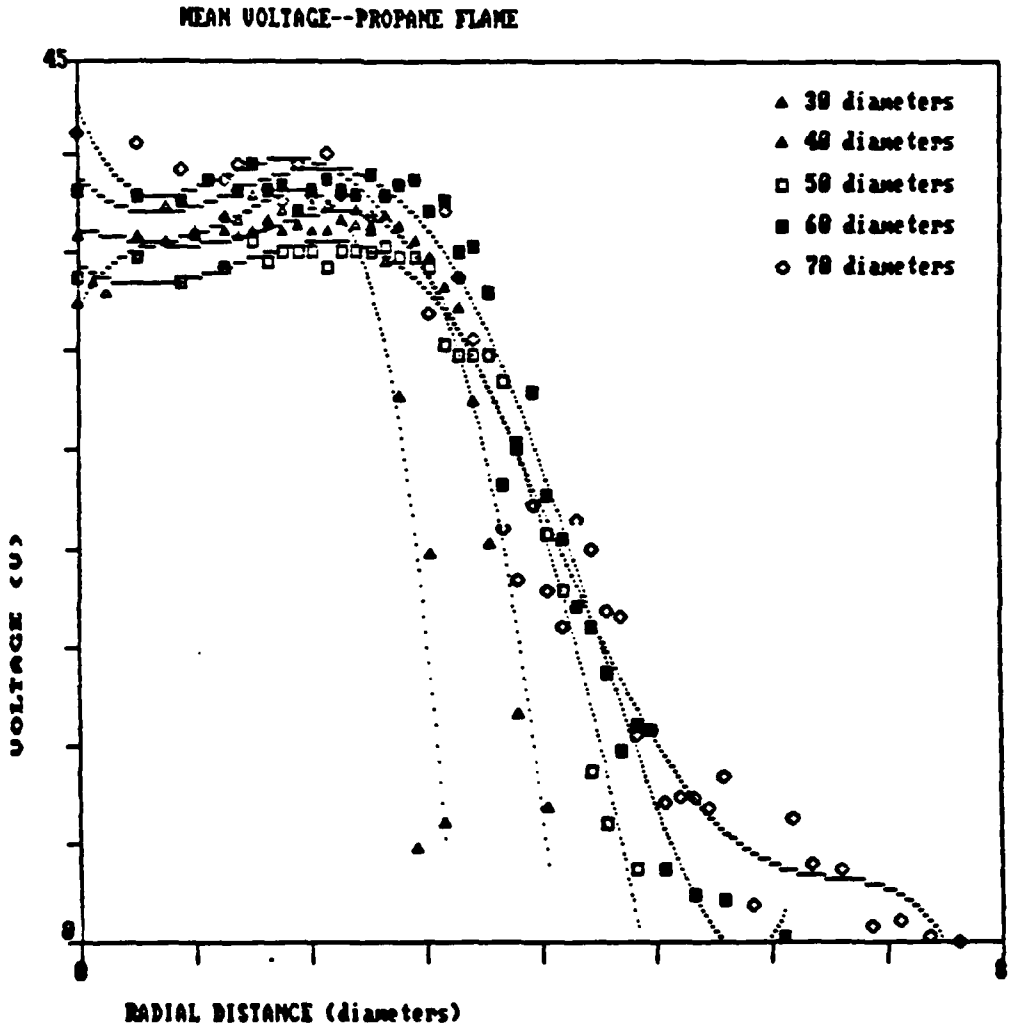
MEAN VOLTAGE--PROPANE FLAME
45
0
VOLTAGE (V)
30 diameters
40 diameters
50 diameters
60 diameters
70 diameters
0
8
RADIAL DISTANCE (diameters)

Figure 41

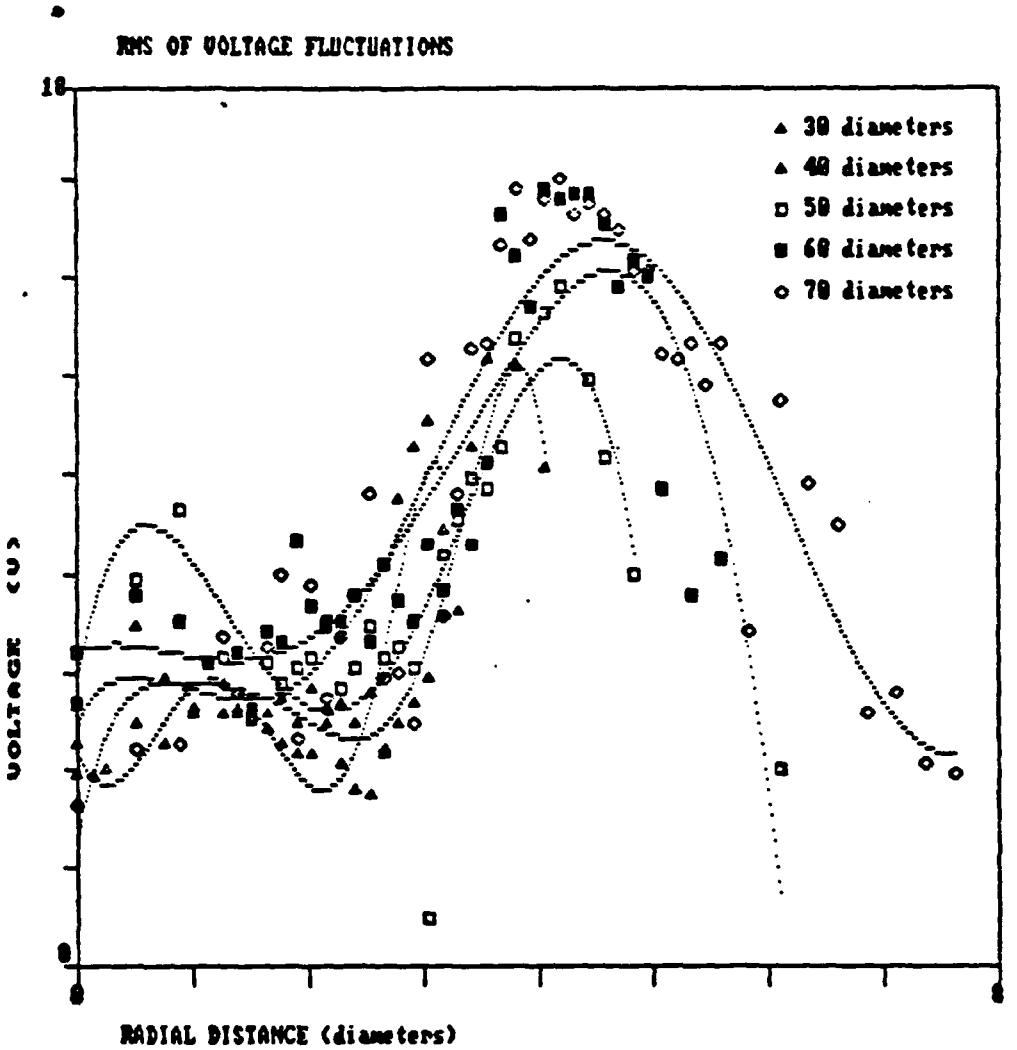
RMS OF VOLTAGE FLUCTUATIONS
18
0
VOLTAGE (V)
30 diameters
40 diameters
50 diameters
60 diameters
70 diameters
0
RADIAL DISTANCE (diameters)

Figure 42

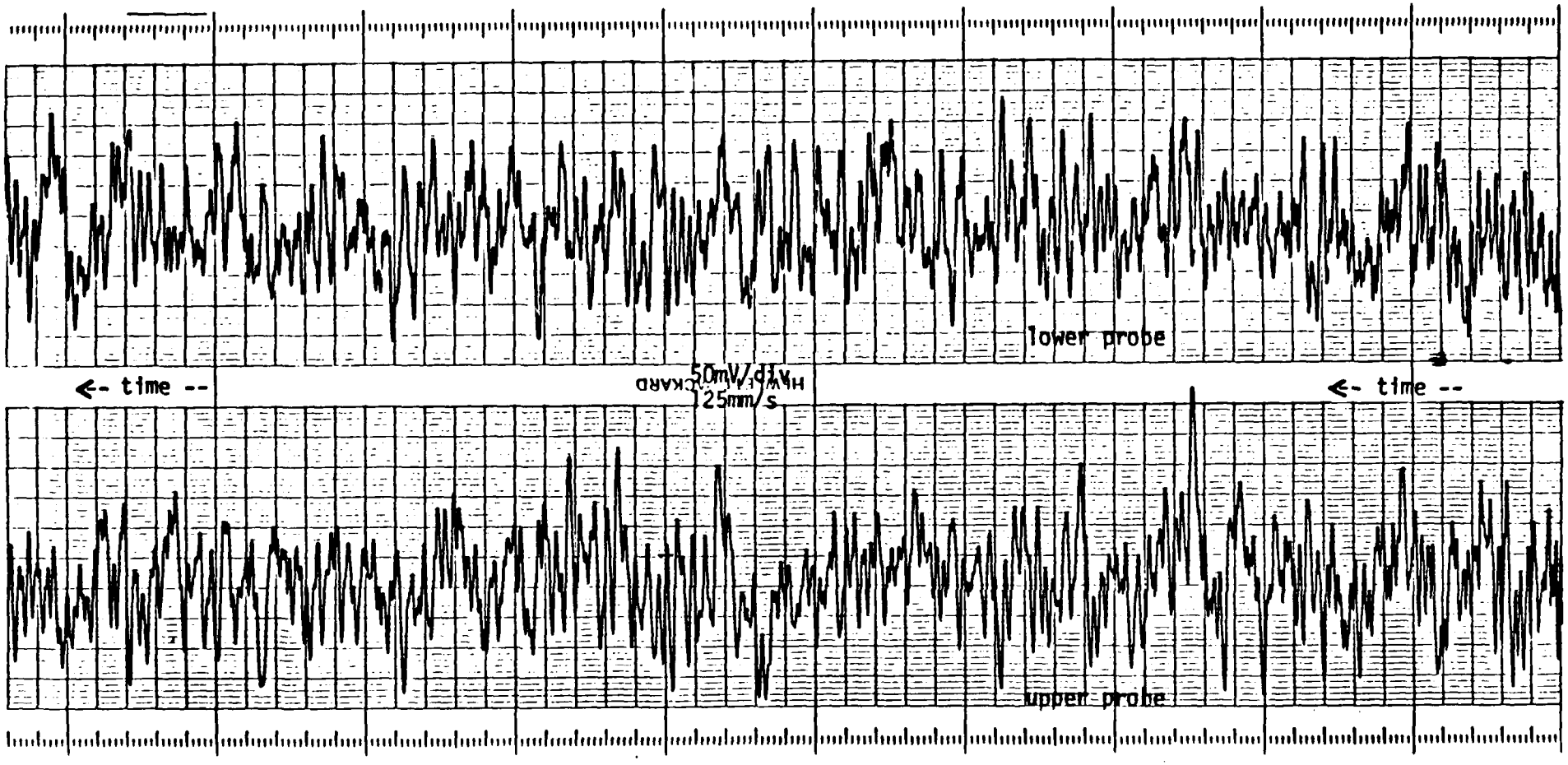

Figure 43

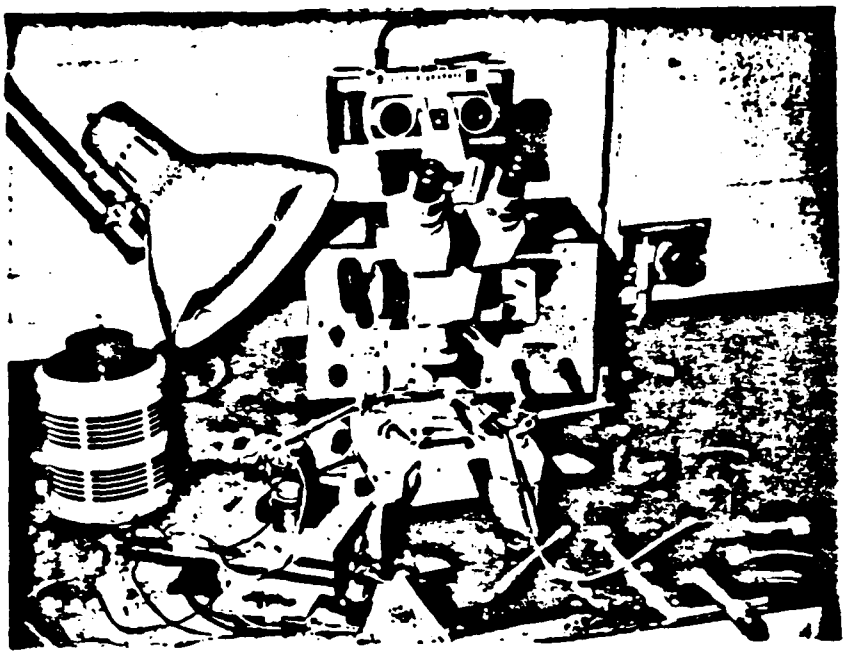

Figure 44

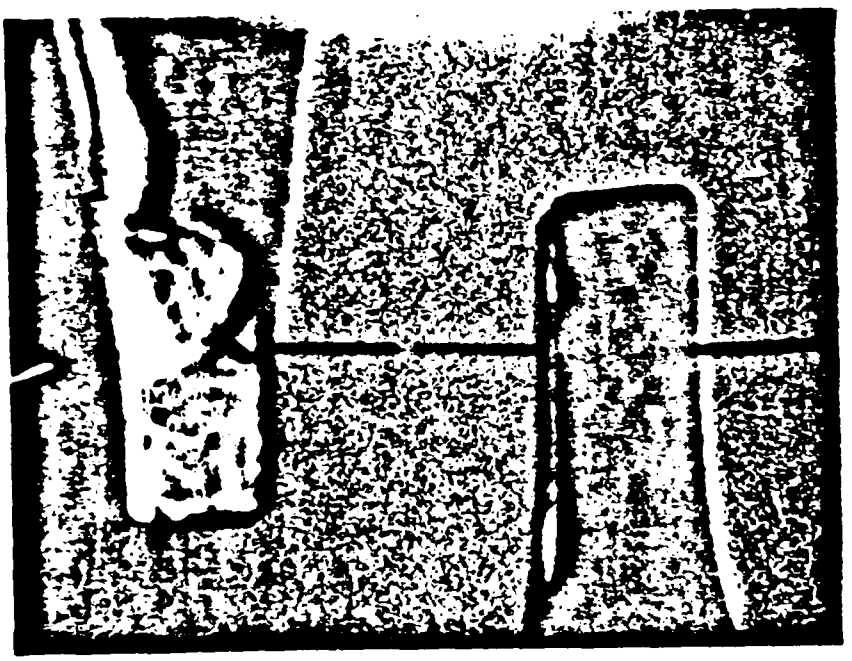

Figure 45

Figure 46

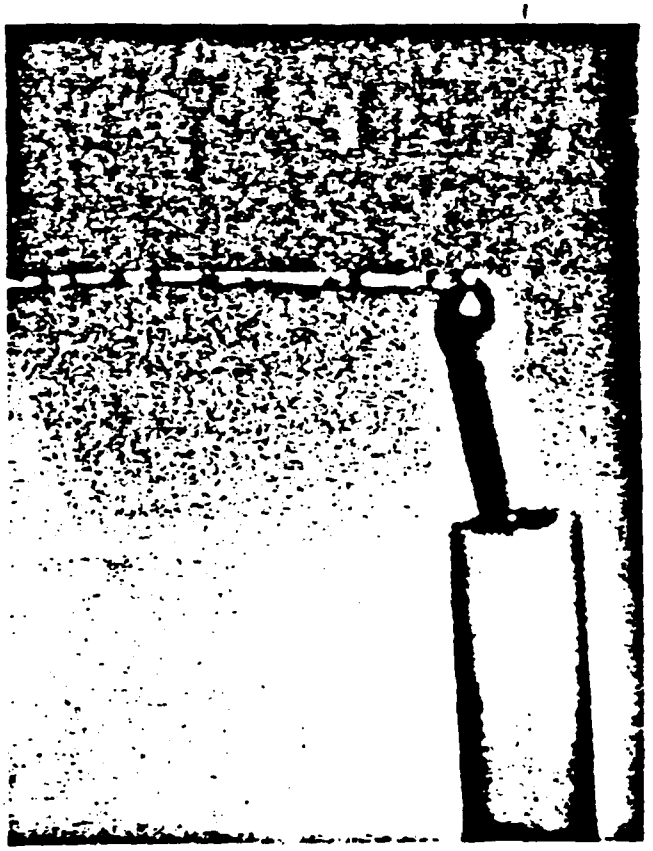

Figure 47

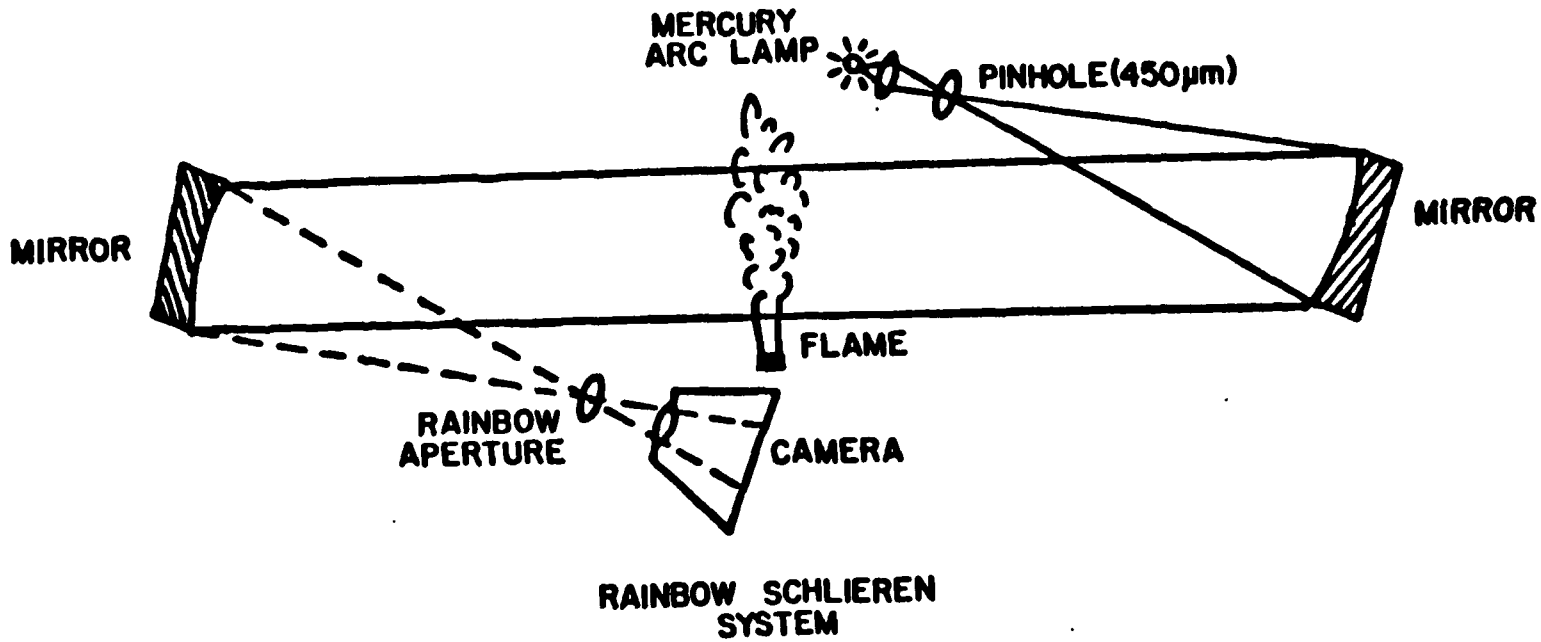
MERCURY
ARC LAMP
PINHOLE(450μm)
MIRROR
MIRROR
FLAME
RAINBOW
APERTURE
CAMERA
RAINBOW SCHLIEREN
SYSTEM

Figure 48

Lifted Methane Flame
Re = 7500

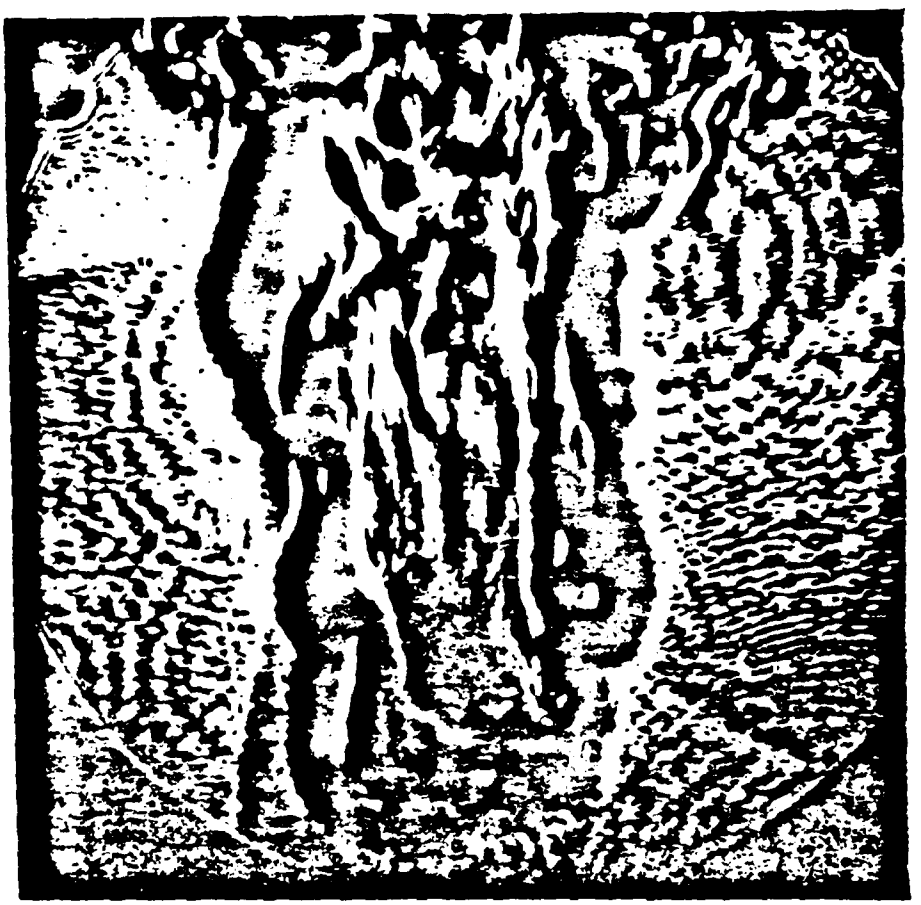

Figure 49

Attached Methane Flames

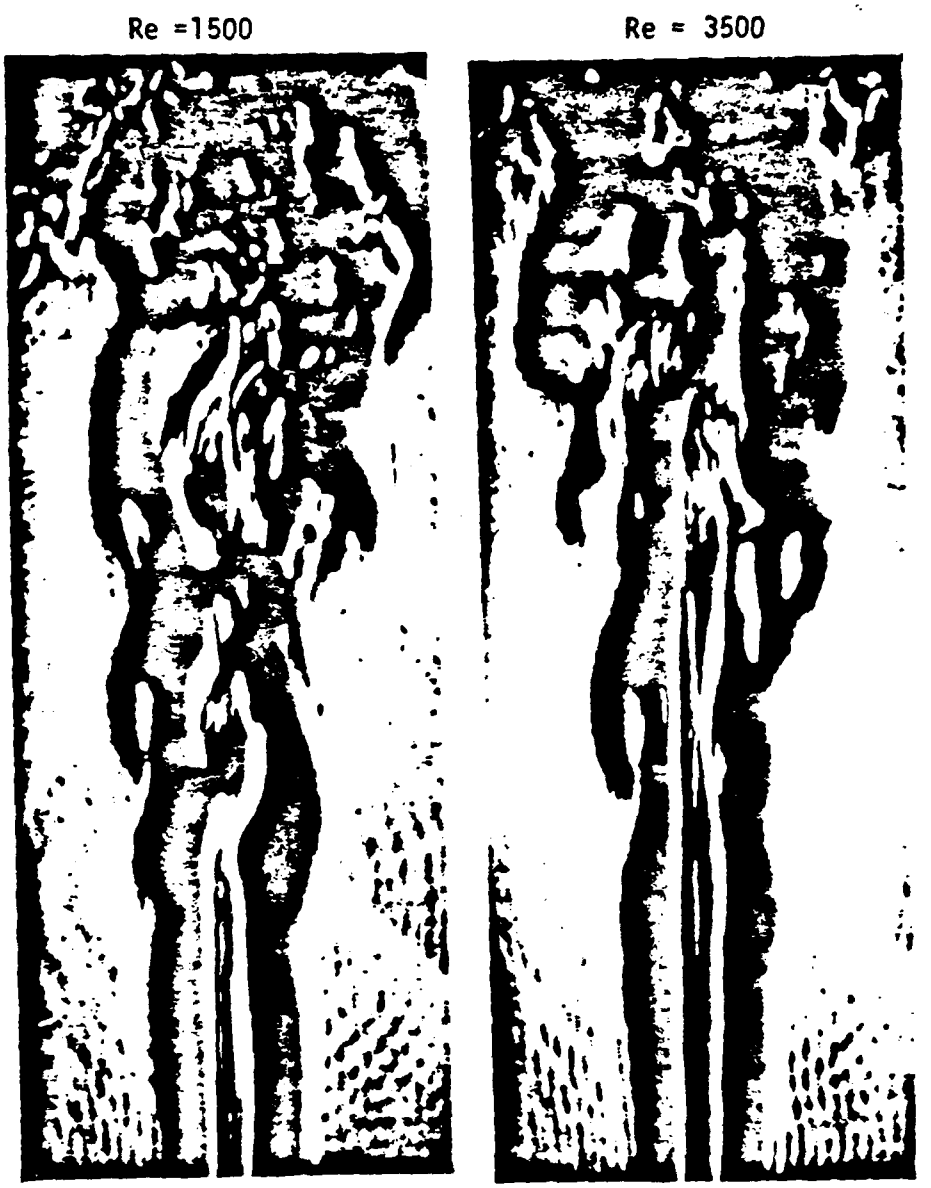

Figure 50

Attached Propane Flame
Re = 9000

Figure 51

END

DTIC

8-86